

1 α ,25-Dihydroxyvitamin D₃ Regulates Mitochondrial Oxygen Consumption and Dynamics in Human Skeletal Muscle Cells^{*[5]}

Received for publication, August 10, 2015, and in revised form, November 19, 2015. Published, JBC Papers in Press, November 24, 2015, DOI 10.1074/jbc.M115.684399

Zachary C. Ryan[‡], Theodore A. Craig[‡], Clifford D. Folmes[‡], Xuewei Wang[§], Ian R. Lanza[‡], Niccole S. Schaible[¶], Jeffrey L. Salisbury^{||}, K. Sreekumaran Nair[‡], Andre Terzic[‡], Gary C. Sieck^{¶||}, and Rajiv Kumar^{‡||1}

From the Departments of [‡]Medicine, [§]Health Sciences Research, [¶]Physiology and Biomedical Engineering, and ^{||}Biochemistry and Molecular Biology, Mayo Clinic College of Medicine, Rochester, Minnesota 55905

Muscle weakness and myopathy are observed in vitamin D deficiency and chronic renal failure, where concentrations of the active vitamin D₃ metabolite, 1 α ,25-dihydroxyvitamin D₃ (1 α ,25(OH)₂D₃), are low. To evaluate the mechanism of action of 1 α ,25(OH)₂D₃ in skeletal muscle, we examined mitochondrial oxygen consumption, dynamics, and biogenesis and changes in expression of nuclear genes encoding mitochondrial proteins in human skeletal muscle cells following treatment with 1 α ,25(OH)₂D₃. The mitochondrial oxygen consumption rate (OCR) increased in 1 α ,25(OH)₂D₃-treated cells. Vitamin D₃ metabolites lacking a 1 α -hydroxyl group (vitamin D₃, 25-hydroxyvitamin D₃, and 24R,25-dihydroxyvitamin D₃) decreased or failed to increase OCR. 1 α -Hydroxyvitamin D₃ did not increase OCR. In 1 α ,25(OH)₂D₃-treated cells, mitochondrial volume and branching and expression of the pro-fusion protein OPA1 (optic atrophy 1) increased, whereas expression of the pro-fission proteins Fis1 (fission 1) and Drp1 (dynamitin 1-like) decreased. Phosphorylated pyruvate dehydrogenase (PDH) (Ser-293) and PDH kinase 4 (PDK4) decreased in 1 α ,25(OH)₂D₃-treated cells. There was a trend to increased PDH activity in 1 α ,25(OH)₂D₃-treated cells ($p = 0.09$). 83 nuclear mRNAs encoding mitochondrial proteins were changed following 1 α ,25(OH)₂D₃ treatment; notably, *PDK4* mRNA decreased, and *PDP2* mRNA increased. *MYC*, *MAPK13*, and *EPAS1* mRNAs, which encode proteins that regulate mitochondrial biogenesis, were increased following 1 α ,25(OH)₂D₃ treatment. Vitamin D receptor-dependent changes in the expression of 1947 mRNAs encoding proteins involved in muscle contraction, focal adhesion, integrin, JAK/STAT, MAPK, growth factor, and p53 signaling pathways were observed following 1 α ,25(OH)₂D₃ treatment. Five micro-RNAs were induced or repressed by 1 α ,25(OH)₂D₃. 1 α ,25(OH)₂D₃ regulates mitochondrial function, dynamics, and enzyme function, which are likely to influence muscle strength.

Vitamin D₃, through the activity of its active metabolite, 1 α ,25-dihydroxyvitamin D₃ (1 α ,25(OH)₂D₃),² is essential for normal calcium and phosphorus balance and the maintenance of skeletal health (1–4). Vitamin D₃ and its metabolites also have important clinical effects on muscle function, the biochemical basis of which is not well understood. Skeletal muscle weakness and myopathy are prominent in humans with vitamin D deficiency, who rapidly respond to treatment with vitamin D₃ (5, 6). Sarcopenia is common in chronic and end stage kidney disease (7, 8), where concentrations of 1 α ,25(OH)₂D₃ are low. The administration of vitamin D₃ has been reported to improve muscle strength in humans (9). Reduced serum 1 α ,25(OH)₂D₃ concentrations have been linked to falls in humans (10, 11), and clinical trials have demonstrated salutary effects of α -calcidol on fall prevention (12). Improvement in muscle fiber size has been documented in elderly subjects treated with 1 α ,25(OH)₂D₃ (13).

Previous reports have shown that in avian and rodent isolated skeletal muscle cells and cultured myoblast cell lines, vitamin D₃ metabolites, such as 25-hydroxyvitamin D₃ (25(OH)D₃) and 1 α ,25(OH)₂D₃, influence cellular calcium and phosphorus uptake, cellular growth, differentiation, and the expression of a limited number of genes (14–19). Many reports suggest that the vitamin D receptor (VDR) is expressed in skeletal muscle (20–24), and VDR deletion in mice results in alterations in muscle function and strength (25, 26). Treatment of vitamin D-deficient humans with cholecalciferol improves muscle phosphocreatine recovery after exercise (27), suggesting that vitamin D₃ or its metabolites alter skeletal muscle oxidative capacity.

To assess the mechanism of action of the active metabolite of vitamin D₃, 1 α ,25(OH)₂D₃, in human skeletal muscle cells, we examined changes in mitochondrial oxygen consumption (OCR), mitochondrial dynamics, mitochondrial OXPHOS proteins, pyruvate dehydrogenase phosphorylation, and nuclear gene expression using whole transcriptome shotgun sequencing (WTSS, RNA-seq) of messenger RNAs and micro-RNAs

^{*} This work was supported by National Institutes of Health Grants HL126451 (to G. C. S.), HL126451 (to C. D. L. F.), DK066013 (to R. K.), and AG009531 (to K. S. N.), Mayo Clinic Grant CCATS UL1TR000135, the Leducq Foundation, and the Mayo Clinic Center for Regenerative Medicine. The authors declare that they have no conflicts of interest with the contents of this article. The content is solely the responsibility of the authors and does not necessarily represent the official views of the National Institutes of Health.

[5] This article contains supplemental Tables 1 and 2.

¹ To whom correspondence should be addressed: MS 1-120, Mayo Clinic, 200 First St. SW, Rochester, MN 55905. Tel.: 507-284-0020; Fax: 507-538-3954; E-mail: rkumar@mayo.edu.

² The abbreviations used are: 1 α ,25(OH)₂D₃, 1 α ,25-dihydroxyvitamin D₃; 25(OH)D₃, 25-hydroxyvitamin D₃; VDR, vitamin D receptor; OCR, oxygen consumption rate; WTSS, whole transcriptome shotgun sequencing; miRNA, microRNA; RNA-seq, mRNA-seq, and miRNA-seq, RNA-, mRNA-, and miRNA-sequencing, respectively; hSkMC, human skeletal muscle cell; qPCR, quantitative PCR; bis-tris, bis(2-hydroxyethyl)iminotris(hydroxymethyl)methane; PDH, phosphorylated pyruvate dehydrogenase; PDK, PDH kinase; 1 α ,24,25(OH)₃D₃, 1 α ,24R,25-trihydroxyvitamin D₃; 24R,25(OH)₂D₃, 24R,25-dihydroxyvitamin D₃; 1 α (OH)D₃, 1 α -hydroxylated vitamin D.

following treatment of cells with 1 α ,25(OH) $_2$ D $_3$. The dependence of the observed changes upon the presence of the VDR was assessed. Our results show extensive 1 α ,25(OH) $_2$ D $_3$ -mediated changes in skeletal muscle mitochondrial OCR, dynamics, pyruvate dehydrogenase phosphorylation, and expression of nuclear genes encoding mitochondrial proteins. These changes suggest important effects on skeletal muscle that are likely to alter skeletal muscle performance.

Experimental Procedures

General—All human studies were by approved by the institutional review board of the Mayo Clinic. 25-Hydroxyvitamin D $_3$, 24(R),25-dihydroxyvitamin D $_3$, 1 α -hydroxyvitamin D $_3$, and 1 α ,25-dihydroxyvitamin D $_3$ were gifts from Dr. Milan Uskokovic (Hoffman-La Roche, Nutley, NJ).

Muscle Biopsies and Mitochondrial Isolation—Muscle biopsies were performed, and mitochondria were isolated as described previously (28, 29).

Cell Culture—Primary human skeletal muscle cells (hSkMCs) were purchased from Lonza (CC-2561) and grown at 37 °C in 5% CO $_2$ in SkM medium (CC-3161). Cells were subcultured at a seeding density of 3500 cells/cm 2 , using Lonza reagents (CC-5034).

Measurement of Oxygen Uptake by Cells—An XF24 extracellular flux analyzer (Seahorse Biosciences) was utilized to measure OCR and glycolytic activity (30). Cells were seeded in a microplate at a density of 3500 cells/well. At ~80% confluence, cells were treated with vitamin D analogs (final concentration, 10 $^{-8}$ M) or ethanol, added 48 h, 24 h, and immediately prior to OCR measurements. OCR was measured following the sequential addition of oligomycin (0.5 μ g/ml), carbonyl cyanide *p*-trifluoromethoxyphenylhydrazone (1 μ M), and rotenone (0.5 μ M)/antimycin A (1 μ M). Baseline respiration rate (basal OCR – rotenone/antimycin A OCR), coupled respiration rate (basal respiration rate – oligomycin OCR), maximal respiration rate (carbonyl cyanide *p*-trifluoromethoxyphenylhydrazone OCR – rotenone/antimycin A OCR), and oxidative reserve (carbonyl cyanide *p*-trifluoromethoxyphenylhydrazone OCR – basal respiration rate) were calculated (31). Oxygen uptake in isolated mitochondria was determined using an Oroboros Oxygraph (Innsbruck, Austria) as described previously (28).

Immunohistochemistry/Microscopy—Skeletal muscle cells were grown on collagen-treated glass plates (MatTek Corp.) and were fixed and treated with VDR antibody as described earlier (32). Skeletal muscle sections (American MasterTech Scientific) were stained with VDR antibody or preadsorbed VDR antibody, as described (32).

Construction of VDR pEGFP Expression Vectors and Transfection into Human Skeletal Muscle Cells—Human VDR cDNA was amplified by PCR with primers with a KpnI site in the 5' primer and BamHI site in the 3' primer. The product was ligated into pEGFP-C1 or pEGFP-N1 (Clontech). HSkMCs were transfected using Lipofectamine 2000 (Life Technologies).

Knockdown of VDR with Silencing RNA—VDR in skeletal muscle cells was knocked down using two Silencer $^{\circ}$ Select siRNAs to the human VDR (siRNA ID s14777 and s14779, Life Technologies). Silencer $^{\circ}$ Select negative control 1 non-

specific siRNA was used in matching cells in equimolar amounts. Lipofectamine (Life Technologies) siRNA complex in Opti-MEM medium was used for transfection. RNA was isolated as detailed below and reverse-transcribed using Superscript III and an oligo(dT) or random hexamer primer, and percentage knockdown of the VDR RNA was determined following quantitative PCR relative to the RPL13A reference gene.

Assessment of Mitochondrial Volume and Fragmentation—To observe dynamic changes in mitochondrial structure, cultured hSkMCs (treated with either vehicle or 1 α ,25(OH) $_2$ D $_3$ for 48 h) were plated on 8-well glass bottom plates (LabTek) and incubated with 100 nM MitoTracker Deep Red (Life Technologies; excitation 638 nm/emission 700 nm) for 15 min at room temperature. Following thorough rinsing with dye-free solution, cells were imaged using a Nikon A1R confocal system (Nikon Instruments Inc.). Images were acquired at 2048 \times 2048 pixels and 12-bit depth using a Plan-Apo \times 60/1.4 numerical aperture oil objective. Images were corrected for background intensity variations using ImageJ software (National Institutes of Health).

For mitochondrial volume measurement, we performed optical sectioning with a 0.5- μ m step. For each cell, mitochondria volume was determined using Nikon Elements software.

Mitochondrial morphometric analysis was performed using procedures developed by Koopman *et al.* (33–35). To assess the extent of filamentous *versus* fragmented morphometry, the form factor (an index of mitochondrial branching) and aspect ratio (an index of mitochondrial branch length) were calculated for each cell using a custom-written MATLAB (The MathWorks)-based program (36, 37). A decrease in aspect ratio and/or form factor indicates mitochondrial fragmentation (33–37).

RNA Preparation for RNA-seq, miRNA-seq, and qPCR—RNA was prepared using RNA/protein spin columns (Clontech).

Digital PCR and Quantitative PCR—Human mRNAs (VDR, CYP24A1, MSTN, PDK4) were quantitated by real-time digital PCR with the QuantStudio $^{\circ}$ three-dimensional digital PCR system using FAM-labeled TaqMan assays. RPL13A was used as a reference gene. Data were analyzed on-line using QuantStudio $^{\circ}$ 3D AnalysisSuite $^{\text{TM}}$ Cloud Software. qPCR for determination of VDR following siRNA knockdown was carried out using a Roche LightCycler 480 qPCR apparatus (Roche Applied Science) with SYBR Green master mix, Universal RT mix (Roche Applied Science), and an intron-spanning qPCR primer pair for the VDR (Roche Applied Science).

Assessment of Mitochondrial Protein Expression Using Western Blotting with Specific Antibodies—We assessed changes in mitochondrial protein expression using antibodies or antibody mixtures (all from Abcam unless otherwise noted) directed against the following mitochondrial proteins or complexes: VDAC1 or porin (ab15895), pyruvate dehydrogenase Western blot antibody mixture (ab110416), pyruvate dehydrogenase E1- α subunit (phosphorylation at position 293) (ab177461), pyruvate dehydrogenase phosphatase 2 (ab133982), pyruvate dehydrogenase kinase 4 (ab71240), total OXPHOS human Western blot mixture (ab110411), mitofusin 1 (ab57602), mitofusin 2 (ab56889), OPA1 (ab42364), Drp-1 (ab56788), and Fis1

(sc-98900, Santa Cruz Biotechnology, Inc.). Human skeletal muscle cells were plated in T175 flasks and treated with vehicle or 1 α ,25(OH) $_2$ D $_3$ (10 $^{-8}$ M) for 48 h. Homogenates of cells were prepared in extraction buffer (ab193970). Cellular protein was quantitated. 15 μ g of cellular protein was treated with SDS-loading buffer containing 20 mM dithiothreitol and loaded on 10% bis-tris polyacrylamide gels. Proteins were separated by electrophoresis and transferred onto PVDF membranes. The membranes were probed with the appropriate primary antibodies at concentrations recommended by the manufacturer. Peroxidase-labeled secondary antibodies were used to generate a chemiluminescent signal that was detected on x-ray film. The intensity of the bands was quantitated using ImageJ software. Equivalence of mitochondrial protein loading was assured by assessing porin intensity.

Measurement of Pyruvate Dehydrogenase in Cell Homogenates—hSkMCs were treated with vehicle ($n = 5$) or 1 α ,25(OH) $_2$ D $_3$, 10 $^{-8}$ M ($n = 6$), for 48 h. Pyruvate dehydrogenase (PDH) activity was measured in 96-well plates with a pyruvate dehydrogenase activity colorimetric assay (BioVision, Milpitas, CA). The increase in absorbance at 450 nm with time was measured. Values for PDH activity were obtained using a standard curve of increasing NADH concentrations.

Assessment of Mitochondrial and Nuclear DNA—Total DNA was prepared from hSkMCs grown in 6-well plates and treated with vehicle (ethanol, $n = 9$) or 10 $^{-8}$ M 1 α ,25(OH) $_2$ D $_3$ ($n = 9$) for 48 h. Confluent cells were lifted using 0.25% trypsin-EDTA, pelleted at 300 $\times g$ in a microcentrifuge, and then resuspended in 200 μ l of Dulbecco's phosphate-buffered saline. DNA was prepared using QIAamp DNA Mini Kit spin columns. DNA was treated with RNase, and purified DNA was eluted from columns into 200 μ l of water. Purified DNA was used to measure the human mitochondrial genes *ND1* and *ND6* and nuclear genes *BECN1* and *NEB* using a NovaQUANTTM human mitochondrial to nuclear DNA ratio kit (EMD Millipore). Quantitative PCR was performed on 2 ng of DNA using specific PCR primers and a Roche LightCycler 480 qPCR apparatus with SYBR Green master I mix (Roche Applied Science). The ratios of mitochondrial genes *ND1* and *ND6* to nuclear genes *BECN1* and *NEB* in cells treated with 10 $^{-8}$ M 1 α ,25(OH) $_2$ D $_3$ or vehicle (ethanol) were determined using crossing points and a standard curve generated with 0.02–20 ng of human DNA.

Preparation of Libraries—mRNA-seq libraries were prepared as described previously (38). RNA libraries were prepared with a TruSeq RNA Sample Prep Kit version 2 (Illumina). Reverse transcription and adaptor ligation steps were performed manually. Poly(A) mRNA was purified from total RNA using oligo(dT) magnetic beads. RNA was treated with RNase-free DNase during preparation of RNAs using the Nucleospin RNA/Protein kit (Clontech). Purified mRNA was fragmented at 95 $^{\circ}$ C for 8 min, eluted from the beads, and primed for first strand cDNA synthesis. The RNA fragments were then copied into first strand cDNA using SuperScript III reverse transcriptase and random primers (Invitrogen). Second strand cDNA synthesis was performed using DNA polymerase I and RNase H. The double-stranded cDNA was purified using a single AMPure XP bead (Agencourt) clean-up step. The cDNA ends

were repaired and phosphorylated using Klenow, T4 polymerase, and T4 polynucleotide kinase followed by AMPure XP bead clean-up. The blunt-ended cDNAs were modified to include a single 3'-adenylate (A) residue using Klenow exo- (3'-5' exo minus). Paired end DNA adaptors (Illumina) with a single "T" base overhang at the 3'-end were immediately ligated to the "A-tailed" cDNA population. Unique indexes, included in the standard TruSeq Kits (12-Set A and 12-Set B) were incorporated at the adaptor ligation step for multiplex sample loading on the flow cells. The adaptor-modified DNA fragments were enriched by 12 cycles of PCR using primers included in the Illumina Sample Prep Kit. The concentration and size distribution of the libraries were determined on an Agilent Bioanalyzer DNA 1000 chip (Santa Clara, CA).

mRNA libraries were loaded onto Illumina TruSeq version 3 paired end flow cells at concentrations of 9 pM to generate cluster densities of 600,000–800,000/mm 2 following Illumina's standard protocol using the Illumina cBot and TruSeq Rapid Paired End Cluster Kit version 3. The flow cells were sequenced as 51 \times 2 paired end reads on an Illumina HiSeq 2000 using the TruSeq SBS Sequencing Kit version 3 and HiSeq data collection version 2.0.12.0 software. Base-calling was performed using Illumina's RTA version 1.17.21.3.

miRNA-seq libraries from total RNA samples were synthesized with a NEBNext[®] multiplex small RNA kit (New England Biolabs) as described previously (39). Adaptors were ligated to the 3'-ends of the small non-coding RNAs present in 500 ng of total RNA. A complementary primer was annealed to the 3'-adaptor sequences, followed by ligation of a 5' RNA adaptor. A cDNA library was created by reverse transcriptase (Superscript III, Invitrogen) treatment of adaptor-ligated and annealed small RNAs. The library was enriched by 15 cycles of PCR employing a common 5' primer and a 3' primer containing one of eight index primers (3'-adaptor complement; index sequences equivalent to Illumina TruSeq Small RNA sequences). The PCR products were purified. The libraries were assessed for miRNA products by Agilent Bioanalyzer DNA 1000 (Santa Clara, CA) analysis. The 130–160-bp region was quantitated to determine equimolar amounts of vehicle and 1 α ,25(OH) $_2$ D $_3$ -treated sample libraries to pool. The pooled small RNA libraries were fractionated to extract an miRNA-enriched sample via 3% Pippin Prep (Sage Science) gel cassettes. Pooled miRNA fractions were assessed by a second Agilent DNA 1000 assay. A predominant peak at 140–150 bp indicated that the miRNA modification and size selection steps were performed as expected. Libraries were loaded onto single end flow cells at concentrations of 8–10 pM to generate cluster densities of 700,000/mm 2 following Illumina's standard protocol using the Illumina cBot cluster kit version 3. The flow cells were sequenced as two reads: 51 cycles using the small RNA sequencing primer (read 1) and an index read to demultiplex the samples. Libraries were sequenced on an Illumina HiSeq 2000 using TruSeq SBS sequencing kit version 3 and SCS version 1.4.8 data collection software. Base calling was performed using Illumina's RTA version 1.12.4.2.

mRNA-seq Data Analysis—mRNA-seq data were processed by the Mayo Bioinformatics Core Facility to identify genes with differential expressions between vehicle- and 1 α ,25(OH) $_2$ D $_3$ -

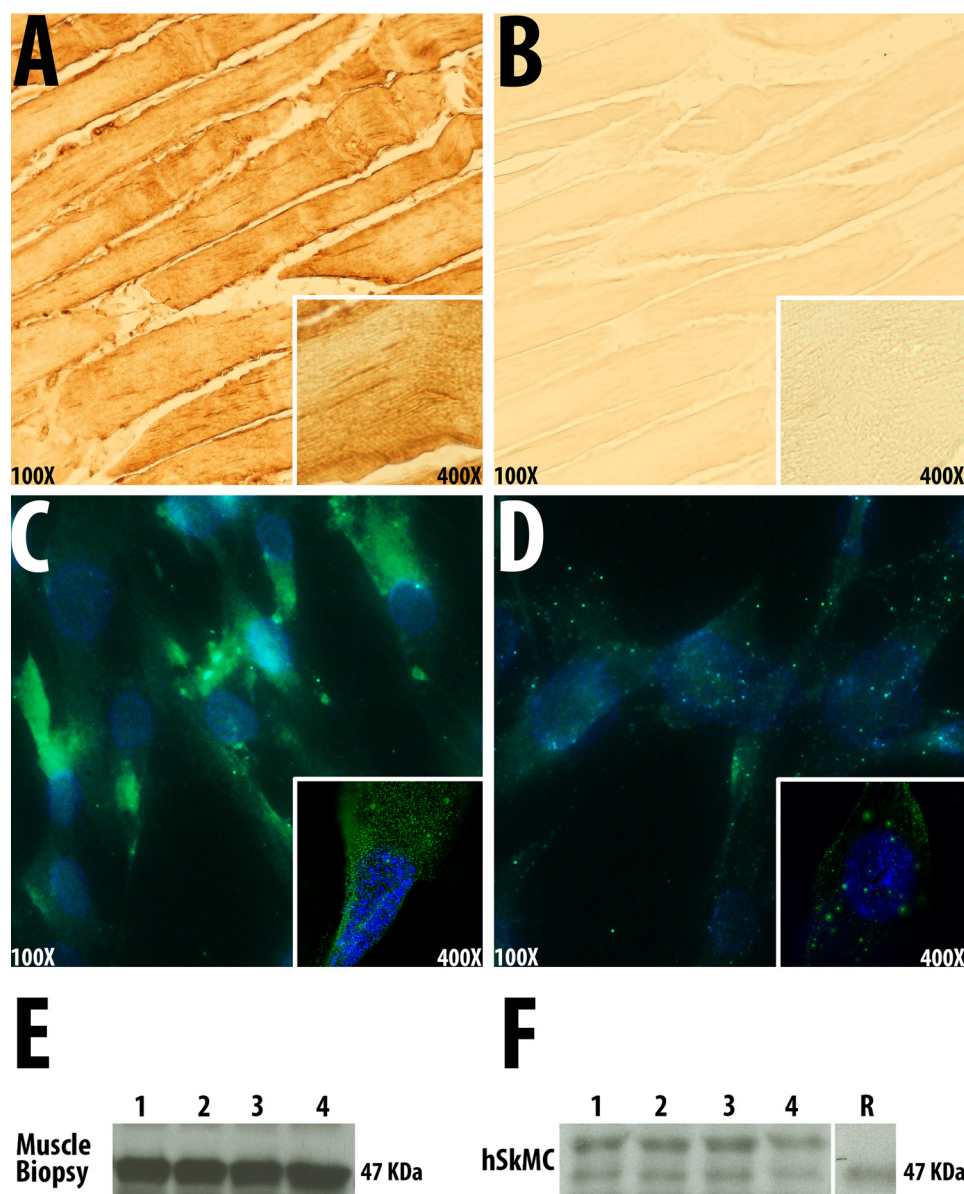


FIGURE 1. The vitamin D receptor is expressed in human muscle and muscle cells. *A*, localization of VDR in sections of normal human skeletal muscle using a polyclonal VDR antiserum (magnification, $\times 100$; *inset* magnification, $\times 400$). *B*, localization of VDR in sections of normal human skeletal muscle using a polyclonal VDR antiserum, preadsorbed with VDR (magnification, $\times 100$; *inset* magnification, $\times 400$). *C*, localization of VDR in primary cultures of human skeletal muscle cells using a polyclonal VDR antiserum (magnification, $\times 100$; *inset* magnification, $\times 630$). *D*, localization of VDR in primary cultures of human skeletal muscle cells using a polyclonal VDR antiserum preadsorbed with VDR (magnification, $\times 100$; *inset* magnification, $\times 630$). *E*, Western blot of homogenates of normal human skeletal muscle tissue obtained by biopsy using a polyclonal VDR antibody. *F*, Western blot of homogenates of primary cultures of human skeletal muscle cells using a polyclonal VDR antibody. *R*, recombinant VDR.

treated groups. The processing of the mRNA data was performed using MAP-RSeq (40) workflow (version 1.2.1.3). MAP-RSeq consists of the following steps: alignment, quality control, obtaining genomic features per sample, and finally summarizing the data across samples. The pipeline provides detailed quality control data across genes using the RSeQC (41) software (version 2.3.2). Paired end reads are aligned by TopHat (42) (version 2.0.6) against the hg19 genome build using the bowtie1aligner (43). Gene counts were generated using HTSeq (44) software (version 0.5.3p9), and the gene annotation files were obtained from Illumina. Differential expression analysis was performed with edgeR version 2.6.2 (45) to identify genes with altered expression by 1 α ,25(OH) $_2$ D $_3$ treatment. A cut-off

for false discovery rate-adjusted *p* value was set at 0.01 to determine the genes with significant expression change between conditions.

miRNA-seq Data Analysis—miRNA-seq data were processed with a microRNA deep sequencing analysis workflow called CAP-miRSeq version 1.1 (46). This workflow provides comprehensive analysis of miRNA sequencing data, including read preprocessing, alignment, mature/precursor/novel miRNA quantification, and variant detection in the miRNA coding region. In particular, CAP-miRSeq utilizes miRDeep2 (47) to classify and quantify the expressions of known and novel miRNAs, based on the annotations from miRBase version 19 (48). Normalization and differential analysis were performed

with edgeR version 2.6.2 (45) to identify known miRNAs with altered expression by 1 α ,25(OH) $_2$ D $_3$ treatment.

miRNA Target Identification—A two-step approach was used to identify potential target genes for the miRNAs differentially expressed between 1 α ,25(OH) $_2$ D $_3$ treatment and control. First, predicted targets were collected from TargetScan version 6.2 (49) for each miRNA. Second, the correlations between differentially expressed miRNAs and mRNAs were evaluated with the Spearman correlation coefficient and its associated statistical significance. The miRNA-mRNA pairs with statistically significant correlation ($p \leq 0.05$) were used to identify target genes. Finally, the common target genes identified by both steps were treated as high confidence targets for each miRNA.

Pathway Analysis—DAVID (version 6.7) (50, 51) was used to perform pathway enrichment analysis for differentially expressed genes or miRNA-targeted genes. DAVID provides pathways from databases, including the Kyoto Encyclopedia of Genes and Genomes (52–54), Panther (55), BioCarta, and Reactome (56). A cut-off p value was set at 0.01 to determine the significantly enriched pathways. The results were further confirmed with Ingenuity Pathway Analysis (Ingenuity Systems).

Analysis of Genes That Encode Mitochondrial Proteins—We specifically examined the differential expression of genes that encode mitochondrial proteins. Mitochondrial proteins were identified based on a compendium from MitoCarta (57). The collection of 1158 nuclear and mitochondrial DNA genes encoding proteins with strong support of mitochondrial localization was searched for differentially expressed genes from 1 α ,25(OH) $_2$ D $_3$ - or vehicle-treated cells.

Statistical Methods—Statistical differences between samples were analyzed using Student's two-tailed t test, assuming equal variance. A p value of <0.05 was regarded as statistically significant.

Data Sharing—All of the sequencing data that were analyzed in this report have been deposited in the Gene Expression Omnibus (GSE70934).

Results

The Vitamin D Receptor Is Expressed in Human Muscle Cells and Skeletal Muscle Homogenates—We confirmed the presence of the VDR in human muscle tissue and hSkMCs by immunohistochemistry. VDR was detected in cellular cytoplasm but not in mitochondria (Fig. 1, A and C). Immunostaining was reduced when VDR preadsorbed antibody was used (Figs. 1, B and D). Western blot analysis with a VDR antibody demonstrated bands of the appropriate mobility ($M_r \sim 48,000$) that co-migrated with recombinant VDR in homogenates of human skeletal muscle biopsies and hSkMC (Fig. 1, E and F). The absence of localization of the VDR in mitochondria was corroborated in cells transfected with a VDR-eGFP expression plasmid, where no mitochondrial localization of fluorescence was noted. We confirmed the presence of the VDR mRNA in muscle cells by isolating mRNA, synthesizing cognate cDNA, and sequencing the VDR mRNA.

1 α ,25(OH) $_2$ D $_3$ Increases Mitochondrial Oxygen Consumption in Adult Human Skeletal Muscle Cells—We measured cellular/mitochondrial OCR following treatment of hSkMCs with 10^{-8} M 1 α ,25(OH) $_2$ D $_3$ or vehicle for 48 h. 1 α ,25(OH) $_2$ D $_3$

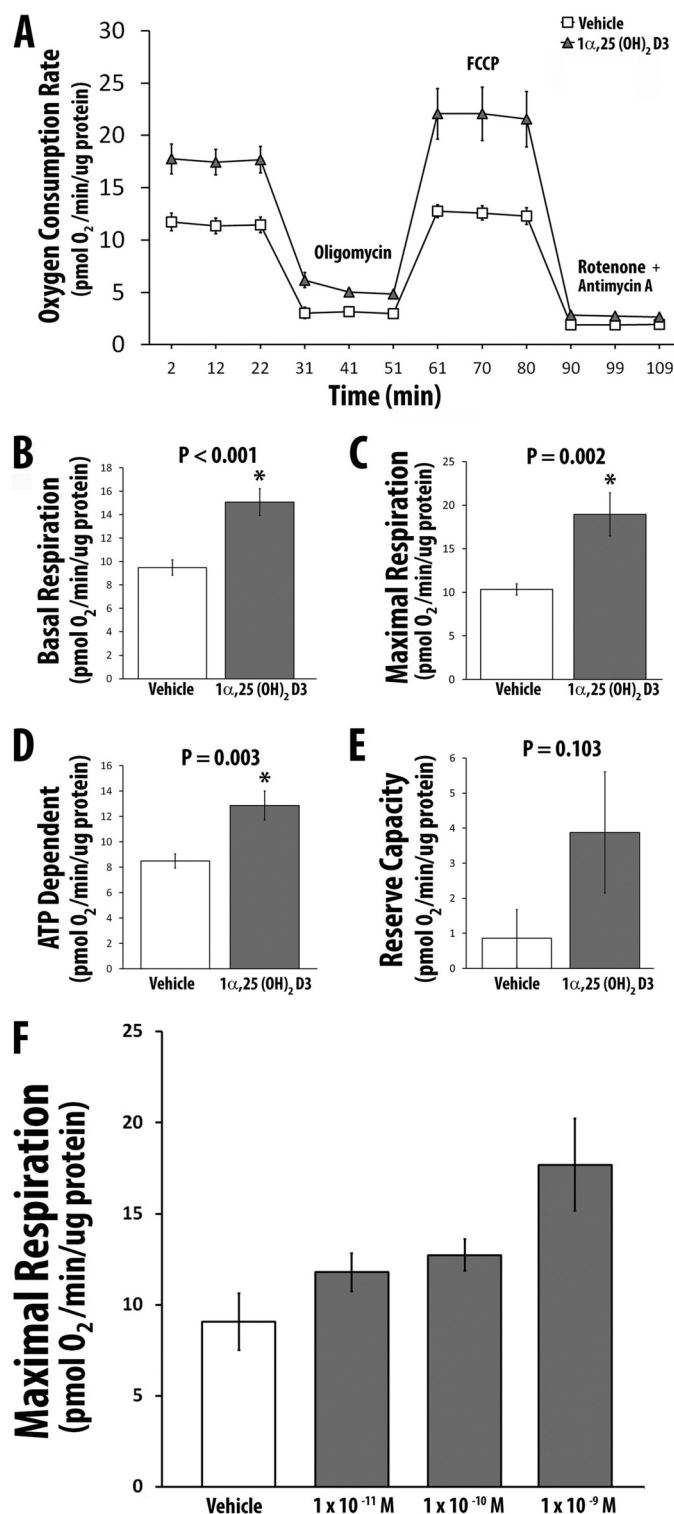


FIGURE 2. 1 α ,25(OH) $_2$ D $_3$ increases cellular OCR in primary cultures of the human skeletal muscle cells. A, OCR in the presence of 1 α ,25(OH) $_2$ D $_3$ ($n = 5$) or vehicle ($n = 8$) and various inhibitors. B, effect of 1 α ,25(OH) $_2$ D $_3$ or vehicle on basal respiration. C, effect of 1 α ,25(OH) $_2$ D $_3$ or vehicle on maximal respiration. D, effect of 1 α ,25(OH) $_2$ D $_3$ or vehicle on coupled respiration. E, effect of 1 α ,25(OH) $_2$ D $_3$ or vehicle on reserve capacity. F, effect of increasing concentrations of 1 α ,25(OH) $_2$ D $_3$ on maximal respiration (vehicle ($n = 3$), 1×10^{-11} M ($n = 4$), 1×10^{-10} M ($n = 4$), 1×10^{-9} M ($n = 3$)). p values (compared with vehicle) for each concentration of 1 α ,25(OH) $_2$ D $_3$ are as follows: 1×10^{-11} M, $p = 0.19$, 1×10^{-10} M, $p = 0.08$, 1×10^{-9} M, $p = 0.04$. All values in A–F are expressed as mean \pm S.E. (error bars).

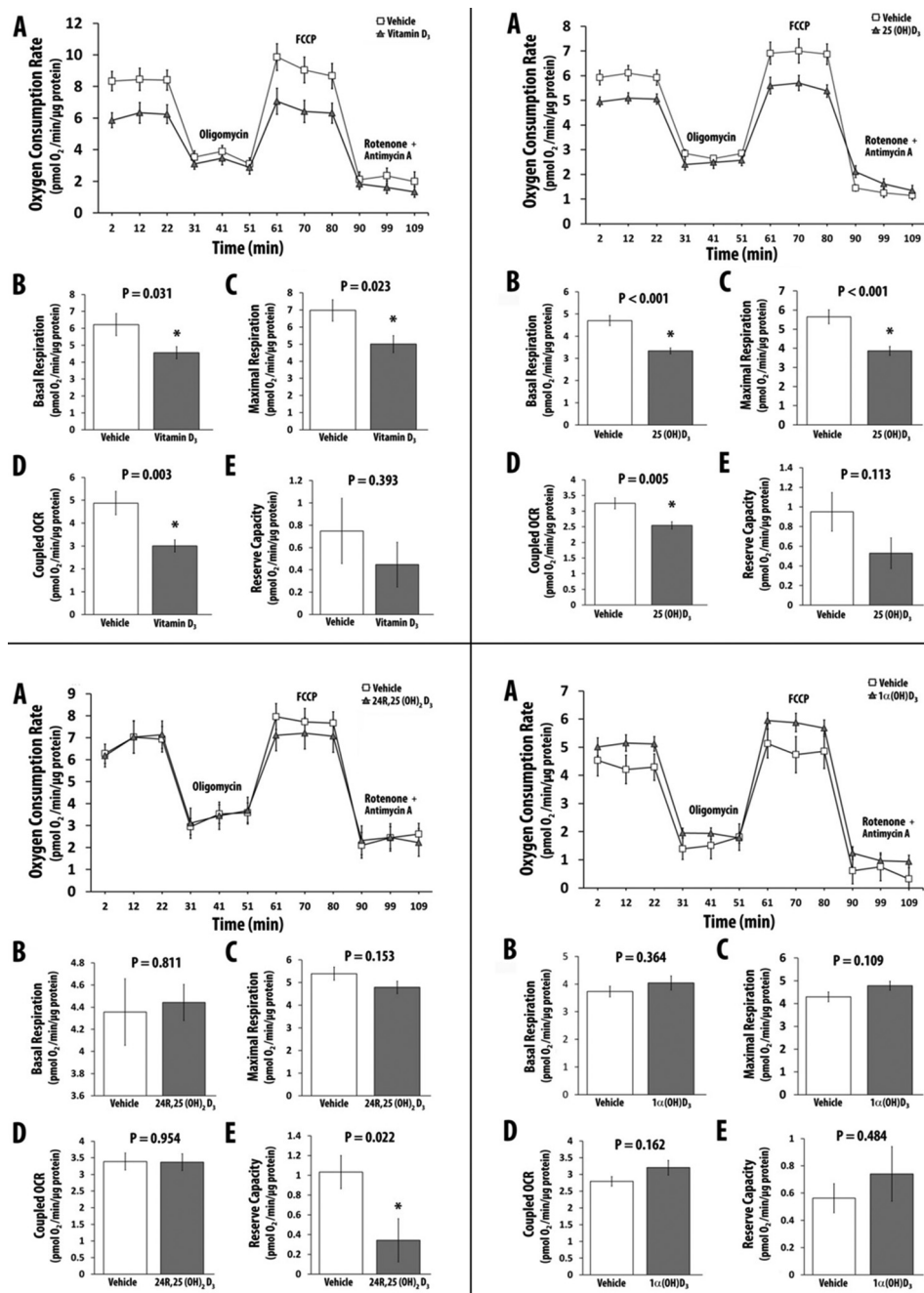


FIGURE 3. The effect of various vitamin D metabolites/analogues on cellular OCR in primary cultures of the human skeletal muscle cells. A, OCR in the presence or absence of vitamin D metabolite and various inhibitors. B, effect of vitamin D metabolite or vehicle on basal respiration. C, effect of vitamin D metabolite or vehicle on maximal respiration. D, effect of vitamin D metabolite or vehicle on coupled respiration. E, effect of vitamin D metabolite or vehicle on reserve capacity. Top left, vitamin D_3 ; top right, $25(\text{OH})\text{D}_3$; bottom left, $24\text{R},25(\text{OH})_2\text{D}_3$; bottom right, $1\alpha(\text{OH})\text{D}_3$. All values in A–E are expressed as mean \pm S.E. (error bars). All replicates had a minimum value of $n = 7$. FCCP, carbonyl cyanide *p*-trifluoromethoxyphenylhydrazone. *, $p \leq 0.05$.

increased basal (standard), coupled (associated with the generation of ATP), and maximal (uncoupled respiration) OCR compared with vehicle (Fig. 2, A–D). Non-mitochondrial OCR was not changed (Fig. 2E). There was a dose-dependent increase in mitochondrial OCR following the addition of increasing amounts of $1\alpha,25(\text{OH})_2\text{D}_3$ to cultures of skeletal muscle cells (Fig. 2F). Simultaneous measurement of OCR and glycolytic activity showed no change in the rate of glycolysis ($1\alpha,25(\text{OH})_2\text{D}_3$ -treated cells = 0.943 ± 0.13 milli-pH units/min/ μg protein versus vehicle-treated cells = 0.763 ± 0.06 milli-pH units/min/ μg protein, $p = 0.213$).

The Increase in Mitochondrial Oxygen Consumption Rate by $1\alpha,25(\text{OH})_2\text{D}_3$ Is VDR-dependent—We treated hSkMCs with either a VDR-specific antisense silencing RNA (siRNA) or a scrambled/control siRNA. Following treatment of cells with VDR siRNA, cellular VDR mRNA decreased by >80%; treatment of cells with control siRNA did change VDR mRNA. Human skeletal muscle cells with reduced VDR expression had decreased basal OCR ($p = 0.002$), maximal respiration ($p = 0.003$), coupled OCR ($p < 0.001$), and respiratory reserve OCR ($p = 0.02$) following $1\alpha,25(\text{OH})_2\text{D}_3$ treatment compared with cells with normal VDR expression. The direct addition of

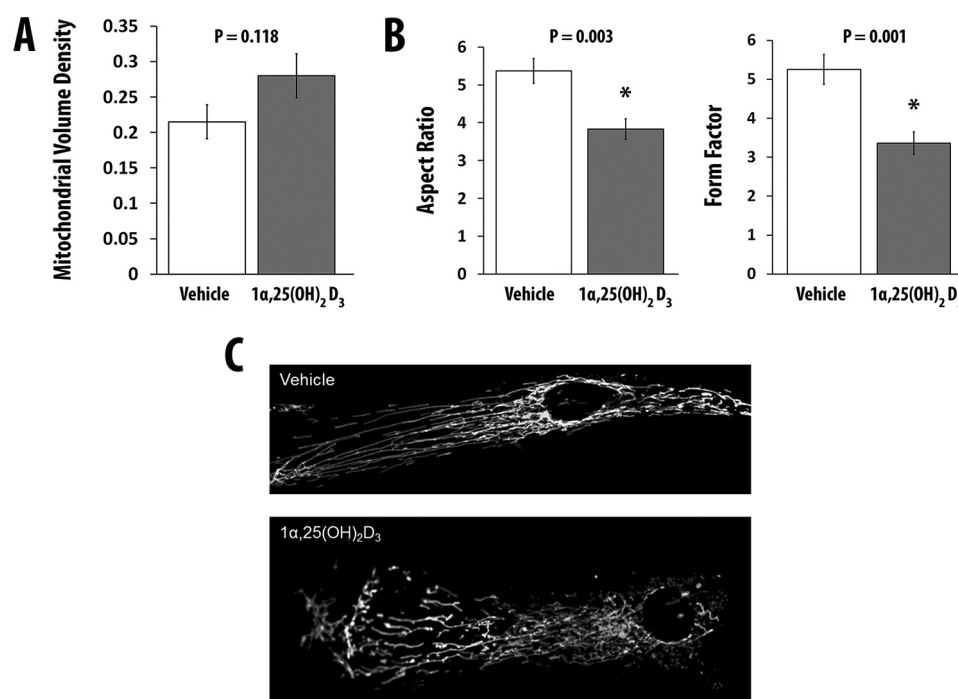


FIGURE 4. **1 α ,25(OH) $_2$ D $_3$ increases mitochondrial volume and fragmentation.** A and B, effect of 1 α ,25(OH) $_2$ D $_3$ or vehicle on mitochondrial volume density (mitochondrial volume normalized to total cell volume) (A) and mitochondrial morphometry (aspect ratio and form factor) (B). C, effect of 1 α ,25(OH) $_2$ D $_3$ or vehicle on mitochondrial ultrastructure. For all measurements, the number of replicates was 10. Values are expressed as mean \pm S.E. (error bars). *, $p \leq 0.05$.

TABLE 1

Quantitation of OPA1, Mfn1, Mfn2, Fis1, and Drp1 proteins

All values are corrected for the expression of porin. Data are expressed as means \pm S.E.

	OPA1	Mfn1	Mfn2	Fis1	Drp1
Vehicle, $n = 4$	0.25 \pm .02	0.41 \pm 0.06	0.57 \pm 0.1	2.16 \pm 0.3	0.69 \pm 0.08
1,25(OH) $_2$ D $_3$, 10^{-8} M, $n = 5$	0.62 \pm 0.1	0.49 \pm 0.05	0.45 \pm 0.02	1.38 \pm 0.15	0.47 \pm 0.06
p	0.01	0.3	0.2	0.04	0.06

1 α ,25(OH) $_2$ D $_3$ to isolated mitochondria failed to increase OCR, suggesting that the effects of 1 α ,25(OH) $_2$ D $_3$ on OCR are dependent on extramitochondrial biochemical events.

C-1 and C-25 Hydroxyl Groups Are Required for Vitamin D $_3$ Analogs to Increase OCR—Both C-1 and C-25 hydroxyl groups are required for optimal binding of vitamin D $_3$ analogs to the VDR (58). To determine the influence of C-1 or C-25 hydroxyl groups or both in vitamin D analogs or metabolites on OCR, we treated hSkMCs with 10^{-8} M vitamin D $_3$, 25(OH)D $_3$, 24R,25(OH) $_2$ D $_3$, or 1 α (OH)D $_3$ for 48 h, following which OCR was determined. Treatment of cells with vitamin D $_3$ (Fig. 3, *top left*) and 25(OH)D $_3$ (Fig. 3, *top right*) decreased maximal OCR; treatment with 24R,25(OH) $_2$ D $_3$ did not change maximal OCR (Fig. 3, *bottom left*), and treatment with 1 α (OH)D $_3$, a 1 α -hydroxylated vitamin D analog, showed a small but statistically insignificant change in OCR (Fig. 3, *bottom right*). The data demonstrate that only 1 α ,25(OH) $_2$ D $_3$ that has both C-1 and C-25 hydroxyl groups and that binds to the VDR with high affinity has a significant effect on OCR in skeletal muscle cells.

1 α ,25(OH) $_2$ D $_3$ Increases Mitochondrial Volume and Branching in Primary Human Skeletal Muscle Cells—We assessed whether 1 α ,25(OH) $_2$ D $_3$ alters mitochondrial volume and branching or fragmentation. We treated hSkMCs with 1 α ,25(OH) $_2$ D $_3$ for 48 h. The volume fraction of mitochondria

(Fig. 4A) and mitochondrial branching increased in cells treated with 1 α ,25(OH) $_2$ D $_3$ (Fig. 4B). As shown in Fig. 4C, 1 α ,25(OH) $_2$ D $_3$ treatment of hSkMCs resulted in morphological changes in mitochondria and a redistribution of mitochondria within the cell.

1 α ,25(OH) $_2$ D $_3$ Increases the Expression of Mitochondrial Proteins That Alter Mitochondrial Fusion and Decreases the Expression of Proteins Associated with Mitochondrial Fission—Treatment of hSkMCs with 1 α ,25(OH) $_2$ D $_3$ increased the expression of OPA1 ($p = 0.01$), a GTPase responsible for fusion of the inner mitochondrial membrane (59–61) (Table 1 and Fig. 5A). Mfn1 and Mfn2, proteins that mediate the fusion of the outer mitochondrial membrane, did not change ($p = 0.30$ and $p = 0.21$, respectively) (Table 1 and Fig. 5B) (59, 60, 62). Concomitantly, 1 α ,25(OH) $_2$ D $_3$ treatment of hSkMCs reduced the expression of Fis1 and DRP-1, proteins that increase mitochondrial fission ($p = 0.04$ and 0.06, respectively) (Table 1 and Fig. 5, C and D) (59, 60, 62). There were no changes in the mRNAs for these proteins on WTSS (see [supplemental Table 1](#)).

1 α ,25(OH) $_2$ D $_3$ Decreases the Expression of Phosphorylated Pyruvate Dehydrogenase and Pyruvate Dehydrogenase Kinase 4—The activity of the PDH complex, located in the outer mitochondrial matrix, regulates the formation of acetyl-CoA from pyruvate and is altered by the phosphorylation status of its E1

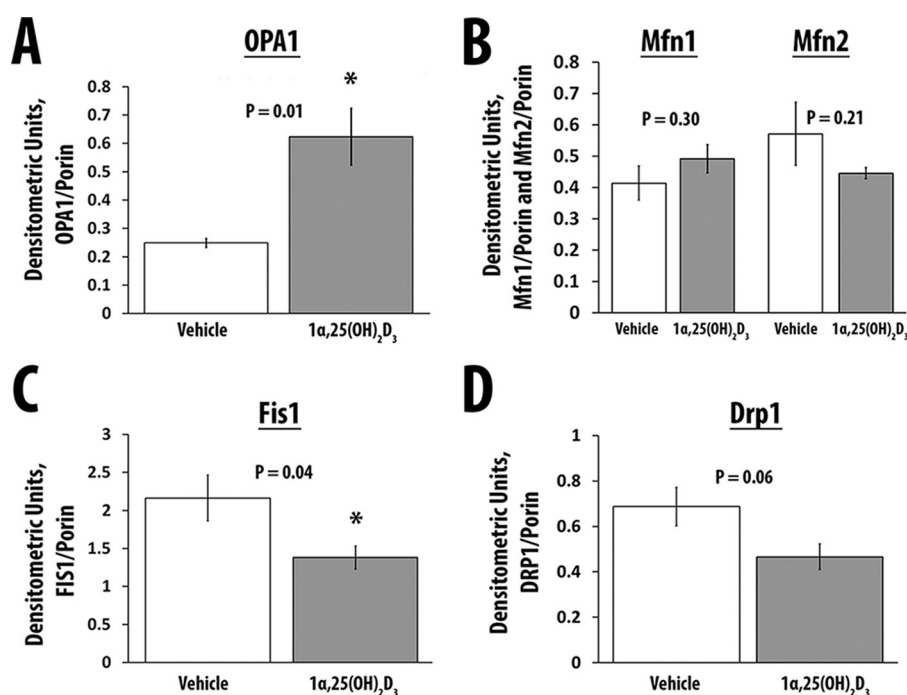


FIGURE 5. The effect of 1 α ,25(OH) $_2$ D $_3$ on the mediators of mitochondrial fusion (OPA1, Mfn1, and Mfn2) and fission (Fis1 and Drp1). A, expression of OPA1 corrected for the expression of Vdac1/porin in cells treated with vehicle ($n = 4$) or 1 α ,25(OH) $_2$ D $_3$ ($n = 5$). B, expression of Mfn1 and Mfn2 corrected for the expression of Vdac1/porin in cells treated with vehicle ($n = 4$) or 1 α ,25(OH) $_2$ D $_3$ ($n = 5$). C, expression of Fis1 corrected for the expression of Vdac1/porin in cells treated with vehicle ($n = 4$) or 1 α ,25(OH) $_2$ D $_3$ ($n = 5$). D, expression of Drp1 corrected for the expression of Vdac1/porin in cells treated with vehicle ($n = 4$) or 1 α ,25(OH) $_2$ D $_3$ ($n = 5$). Values are expressed as mean \pm S.E. (error bars). *, $p \leq 0.05$.

TABLE 2

Quantitation of phospho-PDH E1 (Ser-293), PDK4, and PDP2 proteins

All values are corrected for the expression of porin. Data are expressed as means \pm S.E.

	Phospho-PDH E1 (Ser-293)	PDK4	PDP2
Vehicle, $n = 4$	1.25 \pm .07	0.23 \pm 0.05	0.53 \pm 0.06
1,25(OH) $_2$ D $_3$, 10 $^{-8}$ M, $n = 5$	1.05 \pm 0.04	0.09 \pm 0.03	0.41 \pm 0.05
p	0.04	0.03	0.16

component through the activity of pyruvate dehydrogenase kinases 1–4 (PDK1–4) and pyruvate dehydrogenase phosphatases 1 and 2 (PDP1 and -2) (63–67). Non-phosphorylated PDH is catalytically more active compared with the phosphorylated form of PDH. We observed a decrease in the expression of phosphorylated PDH and PDK4 following treatment of hSkMCs with 1 α ,25(OH) $_2$ D $_3$ ($p = 0.04$ and $p = 0.03$, respectively) (Table 2 and Fig. 6, A and B). Treatment of cells with 1 α ,25(OH) $_2$ D $_3$ was associated with a trend toward an increase ($\sim 13.4\%$) in PDH activity (vehicle, 20.58 \pm 0.19 nmol of NADH/min/mg of protein ($n = 5$); 1 α ,25(OH) $_2$ D $_3$, 23.34 \pm 2.84 nmol of NADH/min/mg ($n = 6$); $p = 0.09$). On WTSS, PDK4 mRNA expression decreased 0.55-fold ($p = 7.21\text{E} - 10$). At the protein level, the expression of the PDH phosphatase, PDP2, tended to increase, but the changes did not reach statistical significance (Table 2 and Fig. 6C, $p = 0.16$). Of note, on WTSS, PDP2 mRNA expression increased 1.2-fold ($p = 2.35\text{E} - 07$).

Effect of 1 α ,25(OH) $_2$ D $_3$ on Mitochondrial DNA/Nuclear DNA Ratios—Treatment of hSkMCs with 1 α ,25(OH) $_2$ D $_3$ did not change the amount of mitochondrial DNA relative to nuclear DNA (mean of ND1 and ND6: 1 α ,25(OH) $_2$ D $_3$ = 2.8 \pm 0.78 ng (mean \pm S.D.) versus vehicle = 2.6 \pm 0.31 ng ($n = 9$))

($p = 0.508$); mean of BECN1 and NEB: 1,25-dihydroxyvitamin D $_3$ = 4.9 \pm 1.39 ng versus vehicle = 3.8 \pm 0.99 ng ($n = 9$) ($p = 0.068$).

1 α ,25(OH) $_2$ D $_3$ Does Not Significantly Alter the Expression of Proteins in the Mitochondrial Respiratory Chain—Treatment of hSkMCs with 1 α ,25(OH) $_2$ D $_3$ did not significantly change proteins in complexes I–V in the mitochondrial respiratory chain (Table 3).

1 α ,25(OH) $_2$ D $_3$ Alters the Expression of Genes Encoding Mitochondrial Proteins, and Genes Encoding Cellular Signaling and Growth-regulatory Pathways in Adult Human Skeletal Muscle Cells—Primary cultures of hSkMCs expressing normal or reduced amounts of the VDR were treated with 1 α ,25(OH) $_2$ D $_3$ or vehicle prior to analysis of gene expression by WTSS. The mRNA-seq data obtained from control or antisense VDR silencing RNA-treated cells, which were subsequently treated with either 1 α ,25(OH) $_2$ D $_3$ or vehicle, showed ~ 400 million total reads with a high degree of correlation of expression profiles (Pearson correlation coefficient = 1); $>95\%$ mRNAs were successfully mapped to known genes (Table 4). Differential gene expression in response to 1 α ,25(OH) $_2$ D $_3$ treatment compared with vehicle with a false discovery rate (or p value adjusted for multiple comparisons) of <0.01 in cells expressing normal VDR concentrations is shown in supplemental Table 1.

853 nuclear mRNAs encoding mitochondrial proteins were detected in primary cultures of human muscle cells. Table 5 lists significantly up-regulated mRNAs, and Table 6 lists significantly down-regulated nuclear mRNAs encoding mitochondrial proteins following treatment with 1 α ,25(OH) $_2$ D $_3$. A 25,000-fold increase in CYP24A1 mRNA expression was seen. Note the decreases in mitochondrial PDK4 (pyruvate dehydro-

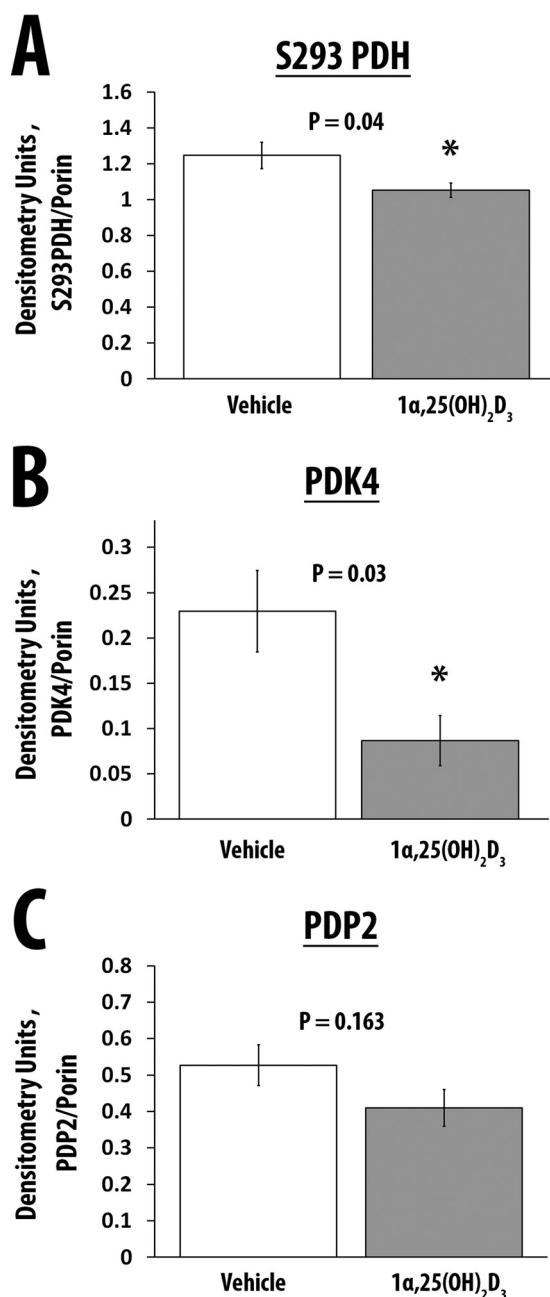


FIGURE 6. The effect of 1 α ,25(OH) $_2$ D $_3$ on the expression of phospho-PDH, PDK4, and PDP2. A, expression of phospho-PDH corrected for the expression of Vdac1/porin in cells treated with vehicle ($n = 4$) or 1 α ,25(OH) $_2$ D $_3$ ($n = 5$). B, expression of PDK4 corrected for the expression of Vdac1/porin in cells treated with vehicle ($n = 4$) or 1 α ,25(OH) $_2$ D $_3$ ($n = 5$). C, expression of PDP2 corrected for the expression of Vdac1/porin in cells treated with vehicle ($n = 4$) or 1 α ,25(OH) $_2$ D $_3$ ($n = 5$). Values are expressed as mean \pm S.E. (error bars).

genase kinase 4) and increases in PDP2 (encoding pyruvate dehydrogenase phosphatase 2) expression. The protein products regulate the activity of pyruvate dehydrogenase that provides acetyl-CoA for the tricarboxylic acid cycle.

We examined RNA-seq data to determine whether the expression of mRNAs known to be involved in mitochondrial biogenesis was altered. Messenger RNAs for MYC, MAPK13, and EPAS1, which encode proteins known to increase mitochondrial biogenesis, were increased following treatment of skeletal muscle cells with 1 α ,25(OH) $_2$ D $_3$. Messenger RNAs for

other factors known to alter mitochondrial biogenesis, such as PGC-1 α , TFAM, AMPK, FOXO3, SIRT1, SIRT3, NRF-1, NRF-2, LKB1, ADRB3, CAV2, CEBPA, COX10, CRYAA, CXADR, DNAJA3, FXN, GNAS, HTT, LETM1, MAN2A1, P2RX7, PRDX3, PTCD2, RAB3A, and SHARPIN were unchanged.

1947 mRNAs (10.2% of \sim 19,000 known human protein-coding genes (68)) are differentially expressed following treatment of muscle cells expressing the VDR with 1 α ,25(OH) $_2$ D $_3$. The most significantly increased mRNA, CYP24A1 (1 α ,25(OH) $_2$ D $_3$ /25(OH) $_2$ D $_3$ -24-hydroxylase; $>25,000$ -fold change, $p = 0$), encodes a mitochondrial cytochrome P450 responsible for the metabolism of 1 α ,25(OH) $_2$ D $_3$ to 1 α ,24,25(OH) $_3$ D $_3$ and conversion of 25(OH) $_2$ D $_3$ to 24R,25(OH) $_2$ D $_3$. Messenger RNAs encoding proteins involved in muscle relaxation (PVALB, parvalbumin, 21.7-fold change, $p = 1.92\text{E}-22$), protein synthesis (IGFN1, Ig-like, fibronectin type III domain-containing 1, 17.5-fold change, $p = 3.22\text{E}-08$), cytoskeletal dynamics (ARHGEF16, ρ guanine nucleotide exchange factor, 10.5-fold change, $p = 1.53\text{E}-06$), RNA and nucleotide binding (TDRD1, tudor domain-containing protein 10, 19.7-fold change, $p = 7.56\text{E}-18$), cellular energy metabolism (IGFL3, insulin growth factor-like 3, 9.5-fold change, $p = 1.59\text{E}-10$), apoptosis (FAIM2, Fas apoptotic inhibitory molecule 2, 6.5-fold change, $p = 5.83\text{E}-22$), and nucleosome function (HIST1H3J, histone cluster 1, H3j, 4.8-fold, $p = 4.16\text{E}-05$) are significantly up-regulated. The most significantly repressed mRNAs encode a calcium-sensitive cysteine protease (CAPN11, calpain 11, 0.10-fold change, $p = 3.92\text{E}-04$) and proteins involved in cell migration (PODN, podocan, 0.29-fold change, $p = 7.82\text{E}-04$) and cellular proliferation (WFDC1, WAP four-disulfide core domain 1, 0.48-fold change, $p = 2.64\text{E}-05$). We confirmed changes in the expression of select mRNAs seen on RNA-seq by measuring select mRNAs by digital PCR or qPCR (Table 7).

Table 8 shows the most significantly changed cellular pathways analyzed with the DAVID (Database for Annotation, Visualization, and Integrated Discovery) program. 1 α ,25-Dihydroxyvitamin D $_3$ -regulated mRNAs encoded cellular proteins involved in focal adhesion, muscle contraction, and signaling through extracellular matrix receptor, integrin, JAK/STAT, MAPK, growth factor, and p53 pathways.

In hSkMCs in which VDR expression was inhibited by anti-VDR siRNA ($>80\%$ inhibition observed), only 15 mRNAs changed following treatment of cells with 1 α ,25(OH) $_2$ D $_3$, compared with 1947 mRNAs altered following treatment of cells with 1 α ,25(OH) $_2$ D $_3$ when the VDR expression is normal. The mRNAs whose expression changed are identical to those altered by 1 α ,25(OH) $_2$ D $_3$ in cells expressing normal amounts of the VDR, but the changes are quantitatively reduced. Knockdown of the VDR in cells resulted in changes in gene expression that were in the opposite direction of those observed following 1 α ,25(OH) $_2$ D $_3$ treatment of VDR-expressing cells (supplemental Table 2).

1 α ,25(OH) $_2$ D $_3$ Alters the Expression of miRNAs in Human Skeletal Muscle Cells—1 α ,25(OH) $_2$ D $_3$ alters the expression of nine miRNAs; of these, five (hsa-miR-143-3p, hsa-miR-133a, hsa-miR-17-5p, hsa-miR-129-5p, and hsa-miR-125b-1-3p) have binding targets in mRNAs that are differentially expressed as a result of 1 α ,25(OH) $_2$ D $_3$ treatment (Table 9). Several signal-

TABLE 3**Quantitation of proteins in respiratory chain complexes I–V**

All values are corrected for the expression of porin. Data are expressed as means \pm S.E. NDUFB8, NADH dehydrogenase (ubiquinone) 1 β subcomplex 8, 19 kDa; SDHB, succinate dehydrogenase complex, subunit B, iron sulfur; UQCR2, ubiquinol-cytochrome c reductase core protein II; COX2, cytochrome c oxidase II; ATP5A, ATP synthase, H $^+$ -transporting, mitochondrial F1 complex α .

	NDUFB8, Complex I	SDHB, Complex 2	UQCR2, Complex III	COX2, Complex IV	ATP5A, Complex V
Vehicle, $n = 4$	1.18 \pm .09	1.09 \pm 0.12	0.65 \pm 0.14	0.49 \pm 0.06	0.73 \pm 0.07
1,25(OH) $_2$ D $_3$, 10 $^{-8}$ M, $n = 5$	1.1 \pm 0.04	0.83 \pm 0.05	0.47 \pm 0.07	0.45 \pm 0.02	0.6 \pm 0.03
p	0.4	0.06	0.25	0.49	0.09

TABLE 4**Overview of mRNA-seq results**

	Normal VDR expression		Inhibited VDR expression	
	Vehicle	1 α ,25(OH) $_2$ D $_3$	Vehicle	1 α ,25(OH) $_2$ D $_3$
No. of total reads	420,947,554 \pm 31,279,048	393,213,995 \pm 42,385,160	387,829,949 \pm 64,716,956	355,215,074 \pm 43,827,913
No. of mapped reads	408,977,138 \pm 31,442,664	381,511,528 \pm 41,785,455	376,167,940 \pm 63,253,459	340,370,655 \pm 40,479,111
Percentage of reads mapped	97.14 \pm 0.26	97.01 \pm 0.23	96.98 \pm 0.11	95.87 \pm 0.77

TABLE 5**Significantly induced mRNAs encoding mitochondrial proteins following treatment of primary human skeletal muscle cells expressing the VDR with 1 α ,25(OH) $_2$ D $_3$**

Gene name	Change	p
	<i>-fold</i>	
<i>CYP24A1</i> , cytochrome P450, 24 A1	25,598	0.00E+00
<i>C15orf48</i> , Chr 15 Orf 48	3.5	1.66E-03
<i>ADHFE1</i> , alcohol dehydrogenase	1.4	9.17E-03
<i>SDSL</i> , serine dehydratase-like	1.4	1.30E-03
<i>SQRDL</i> , sulfide:quinone oxidoreductase	1.4	1.11E-20
<i>HSPB7</i> , heat shock 27 kDa 7	1.4	3.48E-06
<i>SARDH</i> , sarcosine dehydrogenase	1.4	8.55E-04
<i>NTHL1</i> , Nth endonuclease III-like 1	1.3	2.26E-03
<i>OXRI</i> , oxidation resistance protein 1	1.3	2.39E-20
<i>PDP2</i> , pyruvate dehydrogenase phosphatase subunit 2	1.2	2.35E-07
<i>BCAT1</i> , branched chain amino acid transaminase 1	1.2	3.86E-18
<i>AGPAT5</i> , 1-acylglycerol-3-phosphate <i>O</i> -acyltransferase 5	1.2	3.08E-11
<i>HSPA9</i> , heat shock 70-kDa protein 9 (mortalin)	1.19	2.10E-13
<i>GUF1</i> , GTPase homolog	1.19	1.08E-05
<i>SLC25A36</i> , solute carrier family 25, member 36	1.19	1.30E-10
<i>PKD3</i> , pyruvate dehydrogenase kinase, isozyme 3	1.19	3.65E-03
<i>TRIT1</i> , tRNA isopentenyltransferase 1	1.19	2.79E-03
<i>IDH2</i> , isocitrate dehydrogenase 2 (NADP $^+$)	1.14	3.18E-07
<i>SLC16A1</i> , solute carrier family 16 (monocarboxylate transporter), member 1	1.139	1.47E-05
<i>ACADSB</i> , acyl-CoA dehydrogenase, short/branched chain	1.136	9.44E-03
<i>GRPEL2</i> , GrpE-like 2, mitochondrial	1.130	8.47E-03
<i>PTCD3</i> , pentatricopeptide repeat domain 3	1.129	1.31E-04
<i>PDPR</i> , pyruvate dehydrogenase phosphatase regulatory subunit	1.120	2.44E-03
<i>PISD</i> , phosphatidylserine decarboxylase	1.120	8.97E-03
<i>ATAD1</i> , ATPase family, AAA domain-containing 1	1.119	4.90E-04
<i>LRPPRC</i> , leucine-rich pentatricopeptide repeat-containing	1.117	2.92E-05
<i>PPA2</i> , pyrophosphatase (inorganic) 2	1.115	1.27E-03
<i>COQ9</i> , coenzyme Q9	1.114	4.72E-03
<i>MRPS6</i> , mitochondrial ribosomal protein S6	1.114	9.52E-03
<i>PNPT1</i> , polyribonucleotide nucleotidyltransferase 1	1.106	4.50E-03
<i>HSPD1</i> , heat shock 60-kDa protein 1 (chaperonin)	1.098	5.54E-04
<i>ATIC</i> , 5-aminoimidazole-4-carboxamide ribonucleotide formyltransferase/IMP cyclohydrolase	1.094	2.91E-03
<i>HK2</i> , hexokinase 2	1.080	9.42E-03

ing pathways (growth factor, MAPK, integrin) are modulated by these miRNAs through their target mRNAs (Table 10).

Discussion

The salient findings of our report are that 1 α ,25(OH) $_2$ D $_3$ has important effects on mitochondrial physiology, morphology, and expression of key mitochondrial proteins. Mitochondrial OCR increases in skeletal muscle cells treated with 1 α ,25(OH) $_2$ D $_3$. In particular, respiration coupled to the generation of ATP is increased, which suggests that the hormone increases energy production in muscle. The increase in mitochondrial OCR is specific for 1 α ,25(OH) $_2$ D $_3$ that has both C-1 and C-25 hydroxyl groups and does not occur with other vitamin D $_3$ ana-

logs that lack either one of both C-1 and C-25 hydroxyls, such as 25(OH)D $_3$, 25R,25(OH) $_2$ D $_3$, 1 α -(OH)D $_3$, and vitamin D $_3$. The findings are consistent with the high binding affinity of 1 α ,25(OH) $_2$ D $_3$ for the VDR relative to the lower affinities of the other tested analogs (58).

Several mechanisms might account for the increases in mitochondrial OCR. First, increases in mitochondrial volume fraction and branching consistent with mitochondrial fusion and biogenesis (69–72) occur following treatment of muscle cells with 1 α ,25(OH) $_2$ D $_3$. Indeed, there are appropriate increases and decreases in mediators of mitochondrial fusion (OPA1) and fission (Fis1 and Drp1) that are consistent with the observed changes in mitochondrial morphology (59, 60, 62).

TABLE 6Significantly repressed mRNAs encoding mitochondrial proteins following treatment of primary human skeletal muscle cells expressing the VDR with 1 α ,25(OH) $_2$ D $_3$

Gene name	Change	<i>p</i>
	-fold	
<i>PDK4</i> , pyruvate dehydrogenase kinase 4	0.55	7.21E-10
<i>TMEM160</i> , transmembrane protein 160	0.67	6.26E-04
<i>MAOA</i> , monamine oxidase A	0.79	3.46E-12
<i>ELN</i> , elastin	0.79	1.63E-04
<i>PC</i> , pyruvic carboxylase	0.80	1.35E-09
<i>CPT1A</i> , carnitine palmitoyltransferase 1A	0.81	2.67E-05
<i>SNPH</i> , syntrophin	0.82	1.48E-03
<i>COX17</i> , cytochrome <i>c</i> oxidase copper chaperone	0.82	2.18E-03
<i>RAB32</i>	0.82	1.90E-10
<i>HAGH</i> , hydroxyacylglutathione hydrolase	0.82	9.31E-04
<i>ECH1</i>	0.830	8.20E-09
<i>SACSL1</i>	0.831	1.26E-10
<i>ALDH4A1</i> , aldehyde dehydrogenase 4 family, member A1	0.835	7.09E-03
<i>GLRX</i> , glutaredoxin (thioltransferase)	0.847	4.04E-08
<i>PYCR1</i> , pyrroline-5-carboxylate reductase 1	0.847	1.42E-09
<i>DDAH1</i> , dimethylarginine dimethylaminohydrolase 1	0.848	3.53E-09
<i>MRPL41</i> , mitochondrial ribosomal protein L41	0.849	2.68E-03
<i>ATP5D</i> , ATP synthase, H ⁺ transporting, mitochondrial F1 complex, δ subunit	0.853	2.15E-04
<i>ATP10D</i> , ATPase, Class V, Type 10D	0.855	2.70E-06
<i>FASN</i> , fatty acid synthase	0.856	1.23E-05
<i>ACAT2</i> , acetyl-CoA acetyltransferase 2	0.861	1.06E-04
<i>ALKBH7</i> , AlkB, alkylation repair homolog 7	0.861	9.57E-04
<i>TSPO</i> , translocator protein (18 kDa)	0.863	9.13E-05
<i>TAPI</i> , transporter 1, ATP-binding cassette, subfamily B	0.866	3.01E-03
<i>GSR</i> , glutathione reductase	0.874	2.56E-04
<i>AURKAIP1</i> , aurora kinase A-interacting protein 1	0.874	1.87E-04
<i>CYB5R1</i> , cytochrome B5 reductase 1	0.874	6.79E-03
<i>ISOC2</i> , isochorismatase domain-containing 2	0.880	8.18E-03
<i>TSHZ3</i> , teashirt zinc finger homeobox 3	0.882	6.66E-04
<i>FDPS</i> , farnesyl diphosphate synthase	0.884	2.01E-06
<i>RAB1B</i> , member RAS oncogene family	0.888	1.20E-04
<i>PRDX5</i> , peroxiredoxin 5	0.888	6.22E-05
<i>ETFB</i> , electron transfer flavoprotein, β polypeptide	0.891	9.14E-05
<i>NDUFB2</i> , NADH dehydrogenase ubiquinone 1 β subcomplex 2	0.893	1.73E-04
<i>RAB35</i> , member RAS oncogene family	0.894	1.31E-03
<i>PINK1</i> , PTEN-induced putative kinase 1	0.895	1.51E-03
<i>SLC25A1</i> , solute carrier family 25, member 1	0.895	5.36E-04
<i>NDUFA4</i> , NADH dehydrogenase ubiquinone 1 α subcomplex 4	0.898	2.27E-03
<i>OXCT1</i> , 3-oxoacid CoA transferase 1	0.898	3.75E-03
<i>BAX</i> , BCL2-associated X protein	0.900	6.61E-04
<i>PPIF</i> , peptidylprolyl isomerase F	0.902	8.62E-04
<i>FASTK</i> , Fas-activated serine/threonine kinase	0.903	1.26E-03
<i>NME4</i> , NME/NM23 nucleoside diphosphate kinase 4	0.909	1.25E-03
<i>GLUD1</i> , glutamate dehydrogenase 1	0.910	1.22E-03
<i>SLC25A6</i> , solute carrier family 25 (mitochondrial carrier; adenine nucleotide translocator), member 6	0.912	1.96E-03
<i>UXS1</i> , UDP-glucuronate decarboxylase 1	0.913	8.50E-03
<i>COMT</i> , catechol-O-methyltransferase	0.914	9.85E-03
<i>GPX4</i> , glutathione peroxidase 4	0.916	5.34E-03
<i>OAT</i> , ornithine aminotransferase	0.922	7.79E-03
<i>MTCH1</i> , mitochondrial carrier 1	0.925	6.07E-03

TABLE 7

Quantitation of mRNA by digital or quantitative PCR

Data are expressed as mean \pm S.D.

	<i>CYP24A1/RPL13A</i>	<i>VDR/RPL13A</i>	<i>MSTN/RPL13A</i>	<i>PDK4/RPL13A</i>	<i>PVALB/RPL13A</i>
Vehicle, <i>n</i> = 4	0.69 \pm 0.26	0.62 \pm 0.27	1.05 \pm 0.04	1.09 \pm 0.23	0.57 \pm 0.43
1,25(OH) $_2$ D $_3$, 10 ⁻⁸ M, <i>n</i> = 4	34303.4 \pm 2950.21	0.83 \pm 1.02	0.72 \pm 0.17	0.58 \pm 0.07	594.3 \pm 68.1
<i>p</i>	3.59E-05	0.71	0.02	0.007	0.0001

Increases in the mRNA for mediators of increased mitochondrial biogenesis, such as *MYC*, *MAPK13*, and *EPAS1*, are likely to play a role in increasing the numbers of mitochondrial. An increase in mitochondrial volume could account for the increase in mitochondrial OCR (59–62, 73).

Second, we observe decreases in the amount of inactive, phosphorylated pyruvate dehydrogenase following treatment of skeletal muscle cells with 1 α ,25(OH) $_2$ D $_3$. The alterations in the phosphorylation state of PDH are associated with a concomitant decrease in the expression of the PDH kinase, PDK4. There

is a trend toward an increase in the expression of the PDH phosphatase, PDP2. The changes in protein expression are supported by changes in mRNA expression for *PDK4* and *PDP2*. Treatment of cells with 1 α ,25(OH) $_2$ D $_3$ was associated with a trend to an increase in PDH activity (*p* = 0.09). The small increase in PDH complex (PDC) activity could potentially increase the amount of acetyl-CoA entering the tricarboxylic acid cycle and thus might account for an increase in mitochondrial OCR. Insulin is known to decrease PDK4 expression, whereas glucocorticoids have the opposite effect (63, 67, 74–77). In aggregate, the data

suggest that 1 α ,25(OH) $_2$ D $_3$ might regulate carbohydrate and fatty acid metabolism in muscle cells. Confirmation of such effects *in vivo* would be of great interest.

The change in expression of ~2000 nuclear mRNAs, 83 of which encode proteins known to localize in mitochondria following treatment of skeletal muscle cells with 1 α ,25(OH) $_2$ D $_3$, is

TABLE 8

Pathways significantly altered by 1 α ,25(OH) $_2$ D $_3$ treatment of primary human skeletal muscle cells using DAVID analysis and associated databases

Pathway term (gene count)	<i>p</i>	Database
Focal adhesion (61)	7.52E-12	KEGG
ECM-receptor interaction (35)	3.64E-11	KEGG
Integrin signaling (68)	3.15E-10	Panther
Integrin signaling (24)	2.72E-05	Reactome
Gap junction (23)	7.79E-04	KEGG
Axon guidance (30)	6.74E-04	KEGG
Signaling by PDGF (20)	7.06E-05	Reactome
JAK/STAT signaling (10)	0.003	Panther
Pathways in cancer (57)	0.005	KEGG
Signaling by NGF (33)	0.006	Reactome
Regulation of actin cytoskeleton (40)	0.006	KEGG
Metabolism of nucleotides (17)	0.014	Reactome
p53 pathway (16)	0.014	Panther
Interferon-signaling (11)	0.017	Panther
Muscle contraction (9)	0.022	Reactome
Terpenoid backbone biosynthesis (6)	0.028	KEGG
Cell adhesion molecules (24)	0.048	KEGG

TABLE 9

MicroRNAs that are induced or repressed in muscle cells following treatment with 1 α ,25(OH) $_2$ D $_3$

miRNA name	Log $_2$ (-fold change)	<i>p</i>	Differentially expressed target mRNAs	No. of differentially expressed target mRNAs
hsa-miR-143-3p	-1.974	0.010	Yes	13
hsa-miR-133a	-0.987	0.012	Yes	8
hsa-miR-17-5p	-1.258	0.013	Yes	15
hsa-miR-129-5p	0.815	0.015	Yes	279
hsa-miR-532-3p	-0.926	0.017	No	
hsa-miR-501-5p	-0.968	0.025	No	
hsa-miR-618	-1.019	0.037	No	
hsa-miR-1268a	0.719	0.040	No	
hsa-miR-125b-1-3p	0.493	0.046	Yes	72

TABLE 10

Pathways/GO terms significantly enriched in the targets (differentially expressed mRNAs) of miRNAs induced or repressed by 1 α ,25(OH) $_2$ D $_3$

miRNAs	Pathways/gene ontology terms	No. of differentially expressed target genes	<i>p</i>	Database
miR-125b	Golgi stack	3	1.44E-02	GOTERM_CC
miR-125b	Regulation of apoptosis	9	1.53E-02	GOTERM_BP
miR-125b	Regulation of programmed cell death	9	1.62E-02	GOTERM_BP
miR-125b	Regulation of cell death	9	1.65E-02	GOTERM_BP
miR-125b	Nerve growth factor binding	2	2.02E-02	GOTERM_MF
miR-125b	Neurotrophin binding	2	3.22E-02	GOTERM_MF
miR-125b	Positive regulation of membrane protein ectodomain proteolysis	2	3.60E-02	GOTERM_BP
miR-125b	MAPKKK cascade	4	3.88E-02	GOTERM_BP
miR-125b	Identical protein binding	7	4.52E-02	GOTERM_MF
miR-125b	Protein homodimerization activity	5	4.70E-02	GOTERM_MF
miR-125b	Regulation of hydrolase activity	5	4.78E-02	GOTERM_BP
miR-125b	Intrinsic to plasma membrane	10	4.91E-02	GOTERM_CC
miR-125b	Endoplasmic reticulum part	5	4.92E-02	GOTERM_CC
miR-133a	Transmembrane transport	3	3.22E-02	GOTERM_BP
miR-133a	Plasma membrane part	4	3.88E-02	GOTERM_CC
miR-143	Cytoskeletal part	5	6.60E-03	GOTERM_CC
miR-143	Protein domain-specific binding	3	2.07E-02	GOTERM_MF
miR-143	Cytoskeleton	5	2.40E-02	GOTERM_CC
miR-143	Signaling by NGF	3	2.41E-02	REACTOME
miR-143	Positive regulation of DNA binding	2	4.56E-02	GOTERM_BP
miR-129-5p	Integrin signaling pathway	15	4.70E-04	PANTHER
miR-129-5p	ECM-receptor interaction	8	5.62E-04	KEGG
miR-129-5p	Focal adhesion	12	6.19E-04	KEGG
miR-129-5p	Signaling by PDGF	5	6.88E-03	REACTOME
miR-129-5p	Axon guidance	4	2.05E-02	REACTOME
miR-129-5p	Regulation of actin cytoskeleton	9	3.16E-02	KEGG
miR-129-5p	Arrhythmogenic right ventricular cardiomyopathy (ARVC)	5	4.19E-02	KEGG

of interest. In addition to the quantitatively large up-regulation of the mitochondrial *CYP24A1*, mRNAs for other mitochondrial proteins that play a role in carbohydrate and fatty acid metabolism were noted to be either induced or repressed. Of note, a significantly down-regulated mRNA, *PKD4*, encodes the pyruvate dehydrogenase kinase, isoenzyme 4, a serine/threonine kinase that phosphorylates the pyruvate dehydrogenase subunits PDHA1 and PDHA2, and regulates metabolite flux through the tricarboxylic acid cycle (63, 67, 76–78). Conversely, the mRNA for *PDP2*, which encodes pyruvate dehydrogenase phosphatase catalytic subunit 2, is significantly increased. *PDP2* catalyzes the dephosphorylation and concomitant reactivation of the α subunit of the E1 component of the pyruvate dehydrogenase complex (78–80). The changes in the expression of mRNAs for *PDP2* and *PKD4* and documented alterations in the expression of the encoded proteins would function together to increase PDC activity.

The altered mRNAs represent 10.2% of known protein coding genes in the human genome (68). The differentially expressed mRNAs encode proteins that play significant roles in multiple biochemical pathways involved in muscle contraction and relaxation; extracellular matrix-cell receptor interactions; actin cytoskeleton remodeling; and JAK-STAT, insulin-like

growth factor, and p53 signaling. The most profoundly up-regulated mRNA following 1 α ,25(OH) $_2$ D $_3$ treatment of muscle cells is the *CYP24A1* (>25,000-fold increase) that encodes the cytochrome P450 for the 1 α ,25(OH) $_2$ D $_3$ /25(OH)D $_3$ -24-hydroxylase, which catalyzes the transformation of 1 α ,25(OH) $_2$ D $_3$ and 25(OH)D $_3$ to less active metabolites 1 α ,24,25(OH) $_3$ D $_3$ and 24R,25(OH) $_2$ D $_3$. Of note, the mRNA for the calcium-binding protein, parvalbumin, that regulates muscle relaxation is significantly induced by 1 α ,25(OH) $_2$ D $_3$. In addition, the expression of mRNAs encoding several growth factors related to the insulin-like growth factor family and nerve growth factor are up-regulated following treatment of cells with 1 α ,25(OH) $_2$ D $_3$. Pathway analysis indicates the regulation of several factors involved in muscle cellular signaling, apoptosis, and growth. The massive change in mRNA expression following treatment of cells with 1 α ,25(OH) $_2$ D $_3$ is consistent with our earlier findings showing similar large scale, 1 α ,25(OH) $_2$ D $_3$ -mediated changes in mRNA and miRNA expression in *Danio rerio* embryos (38, 39).

The effects of 1 α ,25(OH) $_2$ D $_3$ on mitochondrial OCR may help to explain the observation that reduced serum 1 α ,25(OH) $_2$ D $_3$ concentrations in humans have been linked to falls through reduced muscle strength (10, 11) and that clinical trials have demonstrated salutary effects of 1 α (OH)D $_3$, a 1 α -hydroxylated vitamin D analog that is rapidly metabolized to 1 α ,25(OH) $_2$ D $_3$ *in vivo*, on fall prevention (12). The data also suggest that vitamin D $_3$ and 25(OH)D $_3$ will not be useful in the treatment of muscle weakness unless they are metabolized to 1 α ,25(OH) $_2$ D $_3$, a circumstance that is operative in the context of vitamin D deficiency, where high parathyroid hormone levels drive the rapid metabolism of 25(OH)D $_3$ to 1 α ,25(OH) $_2$ D $_3$. Our findings of increased OCR following treatment of skeletal muscle cells with 1 α ,25(OH) $_2$ D $_3$ are consistent with the report of Sinha *et al.* (27), which showed that treatment of vitamin D-deficient humans with cholecalciferol improves muscle phosphocreatine recovery after exercise, suggesting an effect of 1 α ,25(OH) $_2$ D $_3$ on the formation of high energy phosphorylated intermediates and mitochondrial function. The increase in the numbers of mitochondria could also account for the increase in cellular OCR.

In conclusion, 1 α ,25(OH) $_2$ D $_3$ alters mitochondrial OCR, mitochondrial biogenesis, and PDC activity, demonstrating unique effects of the sterol hormone on muscle biochemistry. In addition, there is a profound change in the expression of several hundred nuclear mRNAs, several of which encode mitochondrial proteins and proteins involved in cell signaling and cell growth. The observed effects could explain the myopathy of vitamin D deficiency that is seen in patients with impaired intake of vitamin D and the myopathy of chronic renal failure, where the production of 1 α ,25(OH) $_2$ D $_3$ is impaired.

Author Contributions—Z. C. R., T. A. C., C. D. F., X. W., I. R. L., N. S. S., and J. L. S. performed the experiments and analyzed the data; K. S. N., A. T., G. C. S., and R. K. designed the experiments and analyzed the data; R. K. wrote the manuscript.

References

- DeLuca, H. F. (2004) Overview of general physiologic features and functions of vitamin D. *Am. J. Clin. Nutr.* **80**, 1689S–1696S
- Haussler, M. R., Haussler, C. A., Bartik, L., Whitfield, G. K., Hsieh, J. C.,

- Slater, S., and Jurutka, P. W. (2008) Vitamin D receptor: molecular signaling and actions of nutritional ligands in disease prevention. *Nutr. Rev.* **66**, S98–S112
- Norman, A. W. (2006) Minireview: vitamin D receptor: new assignments for an already busy receptor. *Endocrinology* **147**, 5542–5548
- Wasserman, R. H., Smith, C. A., Brindak, M. E., De Talamoni, N., Fullmer, C. S., Penniston, J. T., and Kumar, R. (1992) Vitamin D and mineral deficiencies increase the plasma membrane calcium pump of chicken intestine. *Gastroenterology* **102**, 886–894
- Schott, G. D., and Wills, M. R. (1976) Muscle weakness in osteomalacia. *Lancet* **1**, 626–629
- Prineas, J. W., Mason, A. S., and Henson, R. A. (1965) Myopathy in metabolic bone disease. *Br. Med. J.* **1**, 1034–1036
- Foley, R. N., Wang, C., Ishani, A., Collins, A. J., and Murray, A. M. (2007) Kidney function and sarcopenia in the United States general population: NHANES III. *Am. J. Nephrol.* **27**, 279–286
- Domański, M., and Ciechanowski, K. (2012) Sarcopenia: a major challenge in elderly patients with end-stage renal disease. *J. Aging Res.* **2012**, 754739
- Murad, M. H., Elamin, K. B., Abu Elnour, N. O., Elamin, M. B., Alkatib, A. A., Fatourechi, M. M., Almandoz, J. P., Mullan, R. J., Lane, M. A., Liu, H., Erwin, P. J., Hensrud, D. D., and Montori, V. M. (2011) Clinical review: the effect of vitamin D on falls: a systematic review and meta-analysis. *J. Clin. Endocrinol.* **96**, 2997–3006
- Gallagher, J. C., Rapuri, P., and Smith, L. (2007) Falls are associated with decreased renal function and insufficient calcitriol production by the kidney. *J. Steroid Biochem. Mol. Biol.* **103**, 610–613
- Gallagher, J. C. (2004) The effects of calcitriol on falls and fractures and physical performance tests. *J. Steroid Biochem. Mol. Biol.* **89**, 497–501
- Dukas, L., Bischoff, H. A., Lindpaintner, L. S., Schacht, E., Birkner-Binder, D., Damm, T. N., Thalmann, B., and Stähelin, H. B. (2004) Alfacalcidol reduces the number of fallers in a community-dwelling elderly population with a minimum calcium intake of more than 500 mg daily. *J. Am. Geriatr. Soc.* **52**, 230–236
- Ceglia, L., Niramitmahapanya, S., da Silva Morais, M., Rivas, D. A., Harris, S. S., Bischoff-Ferrari, H., Fielding, R. A., and Dawson-Hughes, B. (2013) A randomized study on the effect of vitamin D $_3$ supplementation on skeletal muscle morphology and vitamin D receptor concentration in older women. *J. Clin. Endocrinol. Metab.* **98**, E1927–E1935
- De Boland, A. R., Gallego, S., and Boland, R. (1983) Effects of vitamin D-3 on phosphate and calcium transport across and composition of skeletal muscle plasma cell membranes. *Biochim. Biophys. Acta* **733**, 264–273
- de Boland, A. R., and Boland, R. L. (1984) Effects of vitamin D $_3$ on *in vivo* labelling of chick skeletal muscle proteins with [3H]leucine. *Z. Naturforsch. C* **39**, 1015–1016
- Buitrago, C. G., Ronda, A. C., de Boland, A. R., and Boland, R. (2006) MAP kinases p38 and JNK are activated by the steroid hormone 1 α ,25(OH) $_2$ -vitamin D $_3$ in the C2C12 muscle cell line. *J. Cell. Biochem.* **97**, 698–708
- Buitrago, C. G., Arango, N. S., and Boland, R. L. (2012) 1 α ,25(OH) $_2$ D $_3$ -dependent modulation of Akt in proliferating and differentiating C2C12 skeletal muscle cells. *J. Cell. Biochem.* **113**, 1170–1181
- Girgis, C. M., Clifton-Bligh, R. J., Mokbel, N., Cheng, K., and Gunton, J. E. (2014) Vitamin D signaling regulates proliferation, differentiation, and myotube size in C2C12 skeletal muscle cells. *Endocrinology* **155**, 347–357
- Birge, S. J., and Haddad, J. G. (1975) 25-Hydroxycholecalciferol stimulation of muscle metabolism. *J. Clin. Invest.* **56**, 1100–1107
- Tanaka, M., Kishimoto, K. N., Okuno, H., Saito, H., and Itoi, E. (2014) Vitamin D receptor gene silencing effects on differentiation of myogenic cell lines. *Muscle Nerve* **49**, 700–708
- Srikuea, R., Zhang, X., Park-Sarge, O. K., and Esser, K. A. (2012) VDR and CYP27B1 are expressed in C2C12 cells and regenerating skeletal muscle: potential role in suppression of myoblast proliferation. *Am. J. Physiol. Cell Physiol.* **303**, C396–C405
- Girgis, C. M., Mokbel, N., Cha, K. M., Houweling, P. J., Abboud, M., Fraser, D. R., Mason, R. S., Clifton-Bligh, R. J., and Gunton, J. E. (2014) The vitamin D receptor (VDR) is expressed in skeletal muscle of male mice and modulates 25-hydroxyvitamin D (25OHD) uptake in myofibers. *Endocrinology* **155**, 3227–3237
- Bischoff-Ferrari, H. A., Borchers, M., Gudat, F., Dürmüller, U., Stähelin,

- H. B., and Dick, W. (2004) Vitamin D receptor expression in human muscle tissue decreases with age. *J. Bone Miner. Res.* **19**, 265–269
24. Wang, Y., and DeLuca, H. F. (2011) Is the vitamin D receptor found in muscle? *Endocrinology* **152**, 354–363
25. Endo, I., Inoue, D., Mitsui, T., Umaki, Y., Akaike, M., Yoshizawa, T., Kato, S., and Matsumoto, T. (2003) Deletion of vitamin D receptor gene in mice results in abnormal skeletal muscle development with deregulated expression of myoregulatory transcription factors. *Endocrinology* **144**, 5138–5144
26. Sakai, S., Suzuki, M., Tashiro, Y., Tanaka, K., Takeda, S., Aizawa, K., Hirata, M., Yogo, K., and Endo, K. (2015) Vitamin D receptor signaling enhances locomotive ability in mice. *J. Bone Miner. Res.* **30**, 128–136
27. Sinha, A., Hollingsworth, K. G., Ball, S., and Cheetham, T. (2013) Improving the vitamin D status of vitamin D deficient adults is associated with improved mitochondrial oxidative function in skeletal muscle. *J. Clin. Endocrinol. Metab.* **98**, E509–E513
28. Lanza, I. R., and Nair, K. S. (2009) Functional assessment of isolated mitochondria *in vitro*. *Methods Enzymol.* **457**, 349–372
29. Lanza, I. R., Bhagra, S., Nair, K. S., and Port, J. D. (2011) Measurement of human skeletal muscle oxidative capacity by ³¹P-MR spectroscopy: a cross-validation with *in vitro* measurements. *J. Magn. Reson. Imaging* **34**, 1143–1150
30. Folmes, C. D., Arrell, D. K., Zlatkovic-Lindor, J., Martinez-Fernandez, A., Perez-Terzic, C., Nelson, T. J., and Terzic, A. (2013) Metabolome and metabolome remodeling in nuclear reprogramming. *Cell Cycle* **12**, 2355–2365
31. Folmes, C. D., Martinez-Fernandez, A., Perales-Clemente, E., Li, X., McDonald, A., Oglesbee, D., Hrstka, S. C., Perez-Terzic, C., Terzic, A., and Nelson, T. J. (2013) Disease-causing mitochondrial heteroplasmy segregated within induced pluripotent stem cell clones derived from a patient with MELAS. *Stem Cells* **31**, 1298–1308
32. Kumar, R., Schaefer, J., Grande, J. P., and Roche, P. C. (1994) Immunolocalization of calcitriol receptor, 24-hydroxylase cytochrome P-450, and calbindin D28k in human kidney. *Am. J. Physiol.* **266**, F477–F485
33. Koopman, W. J., Distelmaier, F., Esseling, J. J., Smeitink, J. A., and Willems, P. H. (2008) Computer-assisted live cell analysis of mitochondrial membrane potential, morphology and calcium handling. *Methods* **46**, 304–311
34. Koopman, W. J., Visch, H. J., Smeitink, J. A., and Willems, P. H. (2006) Simultaneous quantitative measurement and automated analysis of mitochondrial morphology, mass, potential, and motility in living human skin fibroblasts. *Cytometry A* **69**, 1–12
35. Koopman, W. J., Visch, H. J., Verkaart, S., van den Heuvel, L. W., Smeitink, J. A., and Willems, P. H. (2005) Mitochondrial network complexity and pathological decrease in complex I activity are tightly correlated in isolated human complex I deficiency. *Am. J. Physiol. Cell Physiol.* **289**, C881–C890
36. Aravamudan, B., Kiel, A., Freeman, M., Delmotte, P., Thompson, M., Vassallo, R., Sieck, G. C., Pabelick, C. M., and Prakash, Y. S. (2014) Cigarette smoke-induced mitochondrial fragmentation and dysfunction in human airway smooth muscle. *Am. J. Physiol. Lung Cell Mol. Physiol.* **306**, L840–L854
37. Delmotte, P., and Sieck, G. C. (2015) Interaction between endoplasmic/sarcoplasmic reticulum stress (ER/SR stress), mitochondrial signaling and Ca²⁺ regulation in airway smooth muscle (ASM). *Can. J. Physiol. Pharmacol.* **93**, 97–110
38. Craig, T. A., Zhang, Y., McNulty, M. S., Middha, S., Ketha, H., Singh, R. J., Magis, A. T., Funk, C., Price, N. D., Ekker, S. C., and Kumar, R. (2012) Research resource: whole transcriptome RNA sequencing detects multiple 1 α ,25-dihydroxyvitamin D₃-sensitive metabolic pathways in developing zebrafish. *Mol. Endocrinol.* **26**, 1630–1642
39. Craig, T. A., Zhang, Y., Magis, A. T., Funk, C. C., Price, N. D., Ekker, S. C., and Kumar, R. (2014) Detection of 1 α ,25-dihydroxyvitamin D-regulated miRNAs in zebrafish by whole transcriptome sequencing. *Zebrafish* **11**, 207–218
40. Kalari, K. R., Nair, A. A., Bhavsar, J. D., O'Brien, D. R., Davila, J. I., Bockol, M. A., Nie, J., Tang, X., Baheti, S., Doughty, J. B., Middha, S., Sicotte, H., Thompson, A. E., Asmann, Y. W., and Kocher, J. P. (2014) MAP-RSeq: Mayo analysis pipeline for RNA sequencing. *BMC Bioinformatics* **15**, 224
41. Wang, L., Wang, S., and Li, W. (2012) RSeQC: quality control of RNA-seq experiments. *Bioinformatics* **28**, 2184–2185
42. Trapnell, C., Pachter, L., and Salzberg, S. L. (2009) TopHat: discovering splice junctions with RNA-Seq. *Bioinformatics* **25**, 1105–1111
43. Langmead, B., Trapnell, C., Pop, M., and Salzberg, S. L. (2009) Ultrafast and memory-efficient alignment of short DNA sequences to the human genome. *Genome Biol.* **10**, R25
44. Anders, S., Pyl, P. T., and Huber, W. (2015) HTSeq: a Python framework to work with high-throughput sequencing data. *Bioinformatics* **31**, 166–169
45. Robinson, M. D., McCarthy, D. J., and Smyth, G. K. (2010) edgeR: a bioconductor package for differential expression analysis of digital gene expression data. *Bioinformatics* **26**, 139–140
46. Sun, Z., Evans, J., Bhagwate, A., Middha, S., Bockol, M., Yan, H., and Kocher, J. P. (2014) CAP-miRSeq: a comprehensive analysis pipeline for microRNA sequencing data. *BMC Genomics* **15**, 423
47. An, J., Lai, J., Lehman, M. L., and Nelson, C. C. (2013) miRDeep*: an integrated application tool for miRNA identification from RNA sequencing data. *Nucleic Acids Res.* **41**, 727–737
48. Griffiths-Jones, S., Grocock, R. J., van Dongen, S., Bateman, A., and Enright, A. J. (2006) miRBase: microRNA sequences, targets and gene nomenclature. *Nucleic Acids Res.* **34**, D140–D144
49. Lewis, B. P., Burge, C. B., and Bartel, D. P. (2005) Conserved seed pairing, often flanked by adenosines, indicates that thousands of human genes are microRNA targets. *Cell* **120**, 15–20
50. Huang da, W., Sherman, B. T., and Lempicki, R. A. (2009) Systematic and integrative analysis of large gene lists using DAVID bioinformatics resources. *Nat. Protoc.* **4**, 44–57
51. Huang da, W., Sherman, B. T., Zheng, X., Yang, J., Imamichi, T., Stephens, R., and Lempicki, R. A. (2009) Extracting biological meaning from large gene lists with DAVID. *Curr. Protoc. Bioinformatics* **10**, 1002/0471250953.bi1311s27
52. Kanehisa, M., Araki, M., Goto, S., Hattori, M., Hirakawa, M., Itoh, M., Katayama, T., Kawashima, S., Okuda, S., Tokimatsu, T., and Yamanishi, Y. (2008) KEGG for linking genomes to life and the environment. *Nucleic Acids Res.* **36**, D480–D484
53. Kanehisa, M., Goto, S., Kawashima, S., Okuno, Y., and Hattori, M. (2004) The KEGG resource for deciphering the genome. *Nucleic Acids Res.* **32**, D277–D280
54. Okuda, S., Yamada, T., Hamajima, M., Itoh, M., Katayama, T., Bork, P., Goto, S., and Kanehisa, M. (2008) KEGG Atlas mapping for global analysis of metabolic pathways. *Nucleic Acids Res.* **36**, W423–W426
55. Mi, H., Guo, N., Kejariwal, A., and Thomas, P. D. (2007) PANTHER version 6: protein sequence and function evolution data with expanded representation of biological pathways. *Nucleic Acids Res.* **35**, D247–D252
56. Joshi-Tope, G., Gillespie, M., Vastrik, I., D'Eustachio, P., Schmidt, E., de Bono, B., Jassal, B., Gopinath, G. R., Wu, G. R., Matthews, L., Lewis, S., Birney, E., and Stein, L. (2005) Reactome: a knowledgebase of biological pathways. *Nucleic Acids Res.* **33**, D428–D432
57. Pagliarini, D. J., Calvo, S. E., Chang, B., Sheth, S. A., Vafai, S. B., Ong, S. E., Walford, G. A., Sugiana, C., Boneh, A., Chen, W. K., Hill, D. E., Vidal, M., Evans, J. G., Thorburn, D. R., Carr, S. A., and Mootha, V. K. (2008) A mitochondrial protein compendium elucidates complex I disease biology. *Cell* **134**, 112–123
58. Revelle, L., Solan, V., Londowski, J., Bollman, S., and Kumar, R. (1984) Synthesis and biologic activity of a C-ring analogue of vitamin D₃: biologic and protein binding properties of 11 α -hydroxyvitamin D₃. *Biochemistry* **23**, 1983–1987
59. Chan, D. C. (2006) Mitochondrial fusion and fission in mammals. *Annu. Rev. Cell Dev. Biol.* **22**, 79–99
60. Chan, D. C. (2012) Fusion and fission: interlinked processes critical for mitochondrial health. *Annu. Rev. Genet.* **46**, 265–287
61. Kao, S. H., Yen, M. Y., Wang, A. G., Yeh, Y. L., and Lin, A. L. (2015) Changes in mitochondrial morphology and bioenergetics in human lymphoblastoid cells with four novel OPA1 mutations. *Invest. Ophthalmol. Vis. Sci.* **56**, 2269–2278
62. Chan, D. C. (2006) Mitochondria: dynamic organelles in disease, aging, and development. *Cell* **125**, 1241–1252
63. Jeong, J. Y., Jeoung, N. H., Park, K. G., and Lee, I. K. (2012) Transcriptional

- regulation of pyruvate dehydrogenase kinase. *Diabetes Metab. J.* **36**, 328–335
64. Krebs, E. G., and Beavo, J. A. (1979) Phosphorylation-dephosphorylation of enzymes. *Annu. Rev. Biochem.* **48**, 923–959
65. Lee, I. K. (2014) The role of pyruvate dehydrogenase kinase in diabetes and obesity. *Diabetes Metab. J.* **38**, 181–186
66. Patel, M. S., Nemeria, N. S., Furey, W., and Jordan, F. (2014) The pyruvate dehydrogenase complexes: structure-based function and regulation. *J. Biol. Chem.* **289**, 16615–16623
67. Roche, T. E., and Hiromasa, Y. (2007) Pyruvate dehydrogenase kinase regulatory mechanisms and inhibition in treating diabetes, heart ischemia, and cancer. *Cell. Mol. Life Sci.* **64**, 830–849
68. Ezkurdia, I., Juan, D., Rodriguez, J. M., Frankish, A., Diekhans, M., Harrow, J., Vazquez, J., Valencia, A., and Tress, M. L. (2014) Multiple evidence strands suggest that there may be as few as 19,000 human protein-coding genes. *Hum. Mol. Genet.* **23**, 5866–5878
69. Iqbal, S., and Hood, D. A. (2014) Oxidative stress-induced mitochondrial fragmentation and movement in skeletal muscle myoblasts. *Am. J. Physiol. Cell Physiol.* **306**, C1176–C1183
70. Khacho, M., Tarabay, M., Patten, D., Khacho, P., MacLaurin, J. G., Guadagno, J., Bergeron, R., Cregan, S. P., Harper, M. E., Park, D. S., and Slack, R. S. (2014) Acidosis overrides oxygen deprivation to maintain mitochondrial function and cell survival. *Nat. Commun.* **5**, 3550
71. Sukhorukov, V. M., Dikov, D., Reichert, A. S., and Meyer-Hermann, M. (2012) Emergence of the mitochondrial reticulum from fission and fusion dynamics. *PLoS Comput. Biol.* **8**, e1002745
72. Ventura-Clapier, R., Garnier, A., and Veksler, V. (2008) Transcriptional control of mitochondrial biogenesis: the central role of PGC-1 α . *Cardiovasc. Res.* **79**, 208–217
73. Chen, H., Chomyn, A., and Chan, D. C. (2005) Disruption of fusion results in mitochondrial heterogeneity and dysfunction. *J. Biol. Chem.* **280**, 26185–26192
74. Frier, B. C., Jacobs, R. L., and Wright, D. C. (2011) Interactions between the consumption of a high-fat diet and fasting in the regulation of fatty acid oxidation enzyme gene expression: an evaluation of potential mechanisms. *Am. J. Physiol. Regul. Integr. Comp. Physiol.* **300**, R212–R221
75. Majer, M., Popov, K. M., Harris, R. A., Bogardus, C., and Prochazka, M. (1998) Insulin downregulates pyruvate dehydrogenase kinase (PDK) mRNA: potential mechanism contributing to increased lipid oxidation in insulin-resistant subjects. *Mol. Genet. Metab.* **65**, 181–186
76. Sugden, M. C., Bulmer, K., Augustine, D., and Holness, M. J. (2001) Selective modification of pyruvate dehydrogenase kinase isoform expression in rat pancreatic islets elicited by starvation and activation of peroxisome proliferator-activated receptor- α : implications for glucose-stimulated insulin secretion. *Diabetes* **50**, 2729–2736
77. Sugden, M. C., Bulmer, K., and Holness, M. J. (2001) Fuel-sensing mechanisms integrating lipid and carbohydrate utilization. *Biochem. Soc. Trans.* **29**, 272–278
78. Thomas, G. W., Mains, C. W., Slone, D. S., Craun, M. L., and Bar-Or, D. (2009) Potential dysregulation of the pyruvate dehydrogenase complex by bacterial toxins and insulin. *J. Trauma* **67**, 628–633
79. Huang, B., Gudi, R., Wu, P., Harris, R. A., Hamilton, J., and Popov, K. M. (1998) Isoenzymes of pyruvate dehydrogenase phosphatase: DNA-derived amino acid sequences, expression, and regulation. *J. Biol. Chem.* **273**, 17680–17688
80. Huang, B., Wu, P., Popov, K. M., and Harris, R. A. (2003) Starvation and diabetes reduce the amount of pyruvate dehydrogenase phosphatase in rat heart and kidney. *Diabetes* **52**, 1371–1376